Quaternary Science Reviews 99 (2014) 60–77

Contents lists available at ScienceDirect

Quaternary Science Reviews

journal homepage: www.elsevier.com/locate/quascirev

Climate in the Western Cordillera of the Central Andes over the last 4300 years

Zbyněk Engel [a, *], Grzegorz Skrzypek [b], Tomáš Chuman [a], Luděk Šefrna [a], Martin Mihaljevič [c]

[a] Charles University in Prague, Faculty of Science, Department of Physical Geography and Geoecology, Albertov 6, 128 43 Praha 2, Czech Republic
[b] University of Western Australia, West Australian Biogeochemistry Centre, John de Laeter Centre of Mass Spectrometry, School of Plant Biology M090, 35 Stirling Highway, Crawley, WA 6009, Australia
[c] Charles University in Prague, Faculty of Science, Institute of Geochemistry, Mineralogy and Mineral Resources, Albertov 6, 128 43 Praha 2, Czech Republic

ARTICLE INFO

Article history:
Received 4 February 2014
Received in revised form
21 May 2014
Accepted 13 June 2014
Available online

Keywords:
Distichia peat
Stable isotope
Palaeoclimate
Late Holocene
Peruvian Andes
South America

ABSTRACT

The *Distichia* peat core obtained in the Carhuasanta valley near Nevado Mismi, Cordillera Chila, provides information on climatic and environmental conditions over the last ~4300 years. The relative changes in the stable carbon isotope composition of plant remains preserved in the core reflect major temperature fluctuations in the Western Cordillera of the southern Peruvian Andes. These temperature variations can be additionally linked with the changes in precipitation patterns by analysing C% and C/N ratio in the core. Relatively warm and moist conditions prevailed from 4280 to 3040 cal. yrs BP (BC 2330–1090) with a short colder dry episode around 3850 cal. yrs BP (BC 1900). The most prominent climate changes recorded in the peat occurred between 3040 and 2750 cal. yrs BP (BC 1090–800) when the initial warming turned to a rapid cooling to temperatures at least 2 °C lower than the mean for the Late Holocene. Initially drier conditions within this event turned to a short wet phase after 2780 cal. yrs BP (BC 830) when the temperature increased again. This event coincides with significant changes in peat and ice core records in the Central Andes matching the timing of the global climate event around 2.8 cal. ka BP. Climatic conditions in the study area became relatively dry and stable after the event for about 800 years. Highly variable temperatures and humidity prevailed during the last 2000 years when an extended warm and relatively humid period occurred between 640 and 155 cal. yrs BP (AD 1310–1795) followed by predominantly colder and drier conditions. The established $\delta^{13}C$ peat record represents the first continuous proxy for the temperature in the southern Peruvian Andes dated by the AMS ^{14}C. *Distichia* peat is wide spread in the Andes and the proposed approach can be applied elsewhere in high altitudes, where no other traditional climate proxies are available.

1. Introduction

The Central Andes extend from 5° to 33°S along the west coast of South America forming a significant topographic barrier for the tropospheric flow. This segment of the Andes also bounds a high-elevated plateau of the Altiplano, which affects the distribution of precipitation and tropical–extratropical interactions (Garreaud et al., 2009; Bershaw et al., 2010). As a result, the Central Andes represent a large area with unique climate conditions, which are related to the location of this area between the tropical and mid-latitude atmospheric circulation systems (May et al., 2011). The climate is modulated by solar radiation and the upper-level circulation that alternates easterly and westerly zonal flow (Garreaud et al., 2003). During austral winter, the easterly winds are restricted to the north of 10°S and the subtropical circulation is dominated by a strong westerly jet causing dry conditions. In summer months, the westerly jet weakens and reaches its southernmost position allowing southward expansion of easterly flow down to 21°S (Garreaud, 2009). The summertime extent of the easterlies is also related with the position of the Intertropical Convergence Zone (ITCZ) and with the position and intensity of an upper tropospheric anticyclone, the Bolivian High, which is induced by deep convection over Amazonia (Lenters and Cook, 1997; Garreaud et al., 2003). The southward transport of moist air from the Amazon Basin and related increase in precipitation over the Central Andes is referred to as the South American Summer

* Corresponding author. Tel.: +420 221 951 373; fax: +420 221 951 367.
E-mail addresses: zbynae@seznam.cz, engel@natur.cuni.cz (Z. Engel).

http://dx.doi.org/10.1016/j.quascirev.2014.06.019
0277-3791/

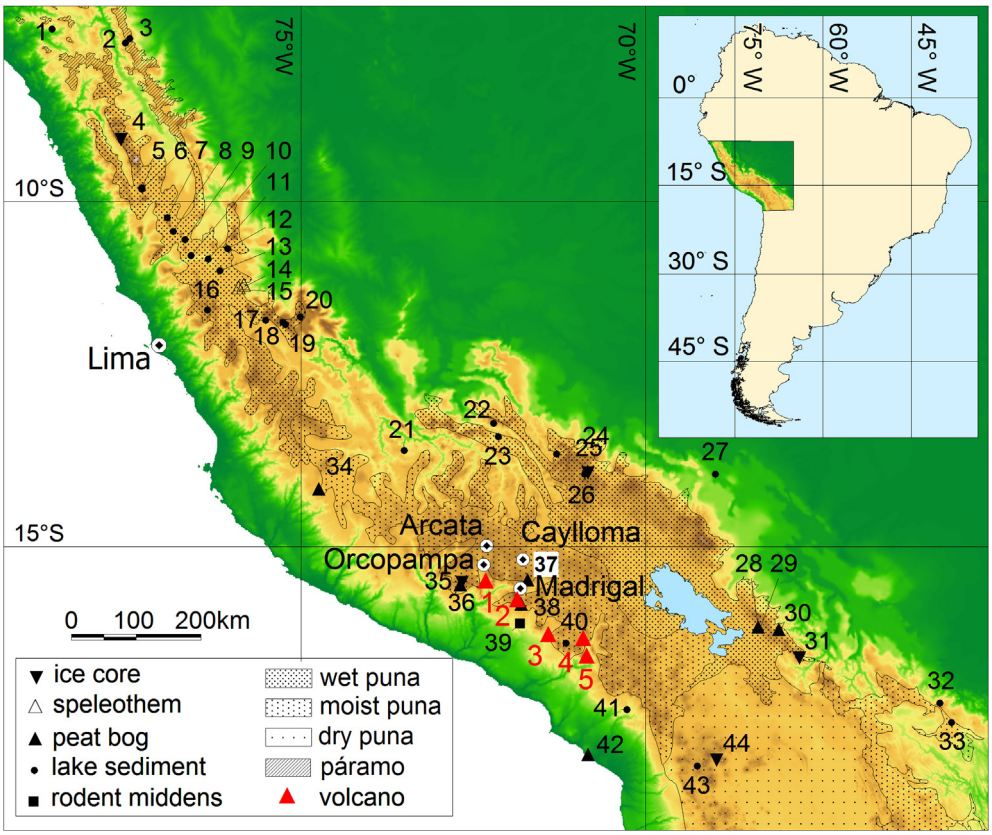

Fig. 1. Location map for the Carhuasanta valley (triangle no. 37) and other paleoclimate records in the Central Andes discussed in this manuscript. Description of locations (numbers 1–44) and references given in Table 1. Red triangles mark volcanoes around the study site. 1 – Chilcayoc, 2 – Sabancaya, 3 – Misti, 4 – Ubinas, 5 – Huaynaputina. (For interpretation of the references to colour in this figure legend, the reader is referred to the web version of this article.)

Monsoon (SASM) (Zhou and Lau, 1998). The variability of the climate system over the Central Andes is affected by the frequency and intensity of El Niño-Southern Oscillation (ENSO), tropical Pacific and Atlantic sea surface temperatures (SST) and other factors, which are still poorly understood (Perry et al., 2014). The location of the Central Andes within large circulation systems explains its climatic sensitivity and makes this mountain area a key site for paleoclimate reconstruction (May et al., 2011; Kanner et al., 2013) as it modulates the atmospheric circulation at meso- to planetary-scale (Seluchi et al., 2006).

Paleoenvironmental studies reveal the climate variation on the Altiplano and Eastern Cordillera over the past 130 ka and 50 ka, respectively (e.g. Kanner et al., 2012; Placzek et al., 2013). Our study expands the range of high-resolution climate proxies to the arid Western Cordillera where no similar data exist. We present the results of stable carbon isotope analyses of *Distichia* peat in a core, which provide a proxy for paleotemperature changes and C% and C/N ratio to illustrate the changes of hydrological regime of the bog as the consequence of variation in precipitation and temperature. The stable carbon isotope composition of *Distichia* peat reflects the mean air temperature of the growing seasons (Skrzypek et al., 2011) that enable us to reconstruct relative temperature variations over the last 4.3 ka. We use this reconstruction to compare paleotemperature changes in the arid western part of the Central Andes with conditions on the Altiplano and in the Eastern Cordillera and to evaluate the trend of temperature in high altitudes of tropics within the Late Holocene. In addition, we analysed the content of metals, lead isotope ratios and magnetic properties of core samples to determine sources of mineral material in the core in relation to climate change. The chronological framework for the temperature record is based on 14 AMS ^{14}C dates.

1.1. Paleoclimate proxies in the Western Cordillera

In order to understand recent and past interconnections between the factors which control the climate in the Central Andes, high-resolution proxies from the boundary locations of this region are needed (e.g. Holmgren et al., 2001; Garreaud et al., 2009). However, within the Central Andes, well-preserved sedimentary records rich in palaeoecological evidence are available mainly from the Altiplano and Eastern Cordillera. Lake-level data and lacustrine deposits from large lakes including Titicaca have been used for reconstructions of paleoenvironmental conditions in the Last Glacial period and Holocene (e.g. Argollo and Mourguiart, 2000; Rowe et al., 2003; Gosling et al., 2008; Fritz et al., 2010). Paleoclimate changes were inferred from sedimentary facies, pollen record, diatom and ostracod assemblages, stable isotopes and archaeological sites (e.g. Cross et al., 2000; Seltzer et al., 2000; Tapia et al., 2003; Grosjean et al., 2007; Placzek et al., 2013). However, sedimentary archives from the Altiplano do not provide evidence for conditions in the semi-arid to arid Western Cordillera. In this range, available proxies are scattered in a wide range of latitude and elevation and their resolution and spatial coverage are low (Fig. 1 and Table 1). Moreover, radiometric chronologies and annually banded records of past climate changes are available only for a few sites in southern Peru (Rodbell et al., 2009; Bromley et al., 2011). Therefore, fossil records suitable for paleoclimate and paleoenvironmental reconstructions are mainly limited to lake sediments, wetland deposits, geomorphological proxies and ice cores.

Andean lakes, salt lake basins and peat bogs mostly contain well-preserved sedimentary record representing a rich archive for paleoenvironmental reconstructions. However, pollen and palaeoecological studies from the Western Cordillera provide data,

Table 1
Palaeoenvironmental records of climate variability in the Central Andes (7–18° S). Geographic locations (1–44) presented on Fig. 1. Radiocarbon ages given as uncalibrated except for data reported by Rodbell et al. (2008).

Site name	Cordillera	Coordinates	Altitude (m a.s.l.)	Record	Length of data series (years)	Dating method	Location on the map (Fig. 1.)	References
La Compuerta	Western	7°30′S, 78°36′W	3950	Lake sediment	47,900 ± 1700	AMS ^{14}C	1	Weng et al., 2006
L. de Chochos	Eastern	7°38′S, 77°28′W	3285	Lake sediment	12,340 ± 110	AMS ^{14}C	3	Bush et al., 2005
L. Baja	Eastern	7°42′S, 77°32′W	3575	Lake sediment	12,100 ± 190	^{14}C	2	Hansen and Rodbell, 1995
Nev. Huascarán	Western	9°6′S, 77°36′W	6048	Ice core	20,000	ALC	4	Thompson et al., 1995, 2000, 2006
Lower Queshquecocha	Western	9°48′S, 77°18′W	4260	Lake sediment	13,130 ± 45	AMS ^{14}C	5	Stansell et al., 2013
Upper Queshquecocha	Western	9°49′S, 77°18′W	4275	Lake sediment	18,440	AMS ^{14}C	6	Rodbell et al., 2008
Jahuacocha	Western	10°14′S, 76°56′W	4076	Lake sediment	7520 ± 110	AMS ^{14}C	7	Stansell et al., 2013
Huarmicocha	Western	10°26′S, 76°50′W	4670	Lake sediment	17,350	AMS ^{14}C	8	Rodbell et al., 2008
Lutacocha	Western	10°33′S, 76°40′W	4320	Lake sediment	8330 ± 160	AMS ^{14}C	9	Stansell et al., 2013
Pumacocha	Eastern	10°41′S, 76°3′W	4300	Lake sediment	11,560 ± 295	AMS ^{14}C	12	Bird et al., 2011a,b
Huatacocha	Western	10°47′S, 76°35′W	4500	Lake sediment	10,050 ± 100	^{14}C	10	Hansen et al., 1984
R. Blanco	Western	10°50′S, 75°20′W	4270	Lake sediment	11,945 ± 150	^{14}C	11	Hansen et al., 1984
L. Junín	W/E	11°00′S, 76°10′W	4100	Lake sediment	39,020 ± 1045	AMS ^{14}C	13	Seltzer et al., 2000
Pacupahuain Cave	Eastern	11°14′S, 75°49′W	3800	Speleothem	48,830 ± 120	^{230}Th	14	Kanner et al., 2012
Huagapo Cave	Eastern	11°16′S, 75°47′W	3850	Speleothem	7111 ± 14	^{230}Th	15	Kanner et al., 2013
L. Milloc	Western	11°34′S, 76°21′W	4325	Lake sediment	10,970 ± 380	^{14}C	16	Graf, 1992
L. Tuctua	Eastern	11°40′S, 75°00′W	4250	Lake sediment	11,360 ± 110	^{14}C	20	Hansen et al., 1994
L. Paca	Western	11°43′S, 75°30′W	3600	Lake sediment	5305 ± 90	^{14}C	17	Hansen et al., 1994
Pomacocha	Eastern	11°45′S, 75°15′W	4450	Lake sediment	9820 ± 130	^{14}C	18	Hansen et al., 1994
L. Jeronimo	Eastern	11°47′S, 75°13′W	4450	Lake sediment	10,960 ± 390	^{14}C	19	Hansen et al., 1994
Marcacocha	Eastern	13°13′S,72°12′W	3355	Lake sediment	3650 ± 60	^{14}C	22	Chepstow-Lusty et al., 2003
L. Huaypo	Eastern	13°25′S, 72°8′W	3500	Lake sediment	3930 ± 30	AMS ^{14}C	23	Mosblech et al., 2012
L. Pacucha	Eastern	13°36′S, 73°30′W	3095	Lake sediment	20,660 ± 90	AMS ^{14}C	21	Hillyer et al., 2009; Valencia et al., 2010
Caserococha	Eastern	13°40′S, 71°17′W	3975	Lake sediment	26,270	AMS ^{14}C	24	Rodbell et al., 2008
Quelccaya	Eastern	13°56′S, 70°50′W	5670	Ice core	1800	ALC	25	Thompson et al., 1985, 2013
Pacococha	Eastern	13°57′S, 70°53′W	4925	Lake sediment	14,440	AMS ^{14}C	26	Rodbell et al., 2008
L. Consuelo	Eastern	13°57′S, 68°59′W	1360	Lake sediment	41,800 ± 570	AMS ^{14}C	27	Bush et al., 2004; Urrego et al., 2010
Cerro Llamoca	Western	14°10′S, 74°44′W	4450	Peat bog	7281 ± 27	AMS ^{14}C	34	Schittek et al., 2014
Q. Carhuasanta	Western	15°29′S, 71°42′W	4809	Peat bog	3771 ± 47	AMS ^{14}C	37	This study
Nev. Coropuna	Western	15°30′S, 72°40′W	6377	Ice core	20,000	^{3}H	35	Vimeux et al., 2009
Nev. Coropuna	Western	15°33′S, 72°41′W	4400	Peat bog	9608 ± 90	AMS ^{14}C	36	Kuentz et al., 2012
R. Sallalli	Western	15°50′S,71°48′W	4400	Peat bog	9650 ± 120	^{14}C	38	Graf, 1999
Q. Chilcane	Western	16°8′–16°16′S, 71°39′–71°49′W	2750	Rodent middens	8560 ± 75	^{14}C	39	Holmgren et al., 2001
Hichu Kkota	Eastern	16°10′S, 68°22′W	4800	Peat bog	4240 ± 85	^{14}C	28	Ostria, 1987; Roux et al., 1987
L. Taypi Chaka Khota	Eastern	16°12′S, 68°21′W	4300	Lake sediment	13,550	AMS ^{14}C	29	Rodbell et al., 2008
Tiquimani	Eastern	16°12′S, 68°4′W	3760	Peat bog	6070 ± 60	AMS ^{14}C	30	Ledru et al., 2013
L. de Salinas	Western	16°24′S,71°9′W	4300	Lake sediment	14,690 ± 200	^{14}C	40	Juvigné et al., 1997; Graf, 1999
Nev. Illimani	Eastern	16°37′S, 67°46′W	6300	Ice core	18,000	ALC, ^{3}H, ^{210}Pb	31	Ramirez et al., 2003; Kellerhals et al., 2010
L. Khomer Kocha Upper	Eastern	17°17′S, 65°44′W	4153	Lake sediment	14,112 ± 61	AMS ^{14}C	32	Williams et al., 2011b
L. Aricota	Western	17°22′S, 70°18′W	2800	Lake sediment	6150 ± 70	AMS ^{14}C	41	Placzek et al., 2001
L. Challacaba	Eastern	17°33′S, 65°34′W	3400	Lake sediment	4471 ± 36	AMS ^{14}C	33	Williams et al., 2011a
Q. de los Burros	Western	18°1′S, 70°50′W	150	Peat bog	8730 ± 70	^{14}C	42	Fontugne et al., 1999
Nev. Sajama	Western	18°6′S, 68°53′W	6542	Ice core	25,000	ALC, ^{3}H, ^{14}C	44	Thompson et al., 1998; Reese et al., 2013
L. Seca	Western	18°11′S, 69°15′W	4500	Lake sediment	7030 ± 245	^{14}C	43	Baied and Wheeler, 1993

which could be only used for rough approximation of temperature conditions in the past. The lower limit of vegetation formations in this region is primarily controlled by seasonal precipitation and temperature is rarely a limiting factor (Latorre et al., 2002). Moreover, only few lakes and bogs were studied in the Western Cordillera. Radiocarbon data and pollen results are available only from a small bog (4400 m a.s.l.) at the foot of Nevado Ampato (35 km south from the study area) and from Lake Salinas (4300 m a.s.l.), which is located 120 km SSE of the area (Juvigné et al., 1997; Graf, 1999). Other published records are based on rodent middens (2350–2750 m a.s.l.) in Arequipa region (Holmgren et al., 2001) and lake sediments (2800–4500 m a.s.l.) in the southern part of the Western Cordillera (Baied and Wheeler, 1993; Hansen et al., 1994; Schwalb et al., 1999; Placzek et al., 2001). Finally, fragmented paleoenvironmental information is available for a few sites in the Western Cordillera of northern Peru and Ecuador (Hansen et al., 1984; Markgraf, 1989; Graf, 1992; Rodbell et al., 1999, 2008; Weng et al., 2004, 2006; Stansell et al., 2013). All these records represent relatively low elevation compared to our core site in the Carhuasanta valley (Table 1).

Glaciers in the Western Cordillera are moisture-limited and their activity is probably related to temporal changes in precipitation (Kaser, 2001). A decrease in temperature has little effect on mass balance of these glaciers, which already lie above the 0 °C isotherm (Rodbell et al., 2009). With respect to the increased sensitivity of glaciers to moisture, the paleotemperature implications of reconstructed glaciation changes in the past have to be considered with caution. Regional glaciation histories, former and modern equilibrium line altitudes were reconstructed in a few areas of the Western Cordillera (Hastenrath, 1967; Clapperton,

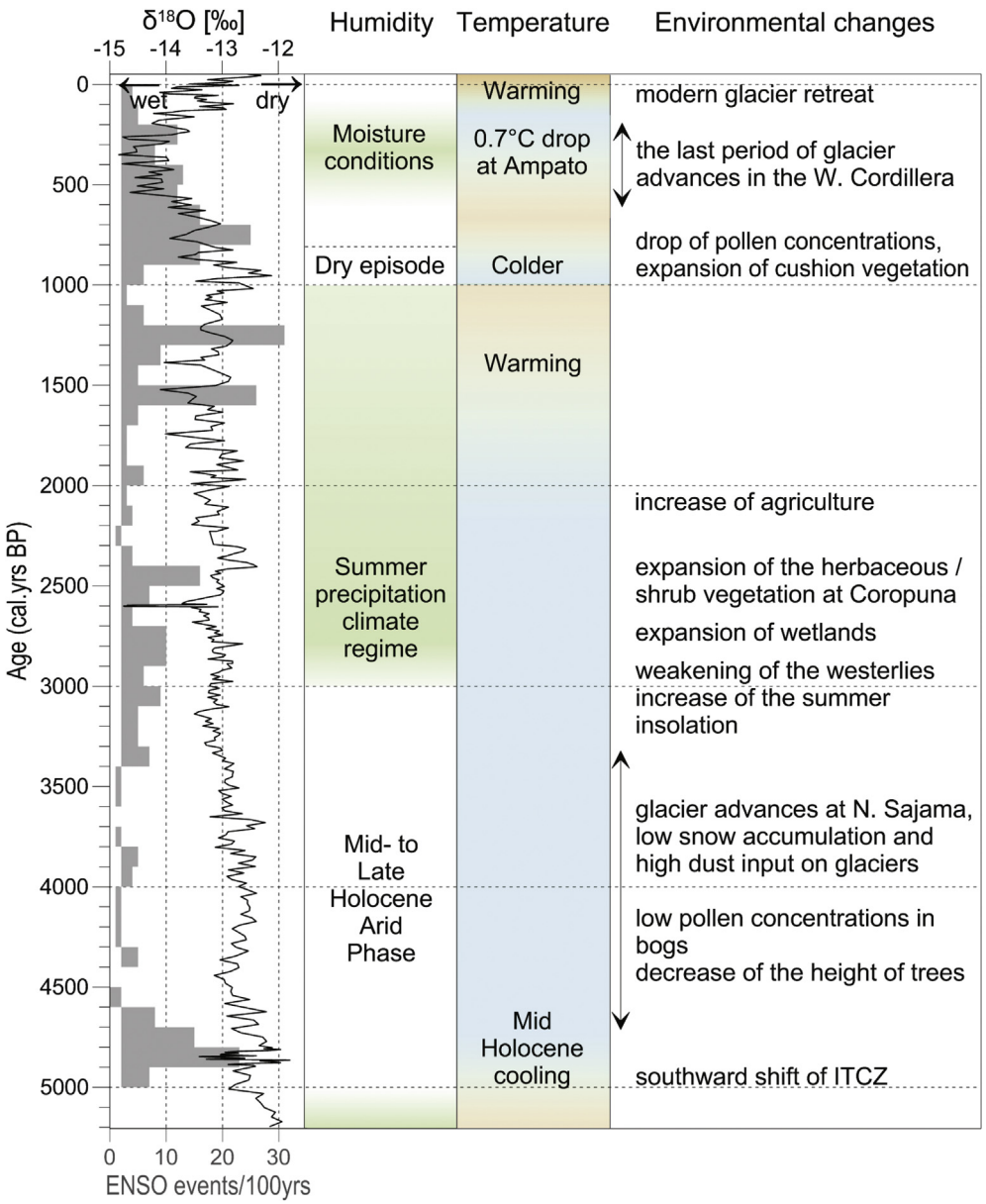

Fig. 2. Paleoclimate conditions in the Western Cordillera of the Central Andes in the last 5000 years. The number of ENSO events per 100 years adopted from Moy et al. (2002), Pumacocha stable oxygen isotope data from Bird et al. (2011b). Climate and environmental changes in the Central Andes described according to Holmgren et al. (2001), Thompson et al. (2006), Jomelli et al. (2009), Smith et al. (2009), Alcalá et al. (2010) and Kuentz et al. (2012).

1983; Rodbell, 1992; Kull and Grosjean, 2000; Dornbusch, 2002; Solomina et al., 2007; Jomelli et al., 2009; Smith et al., 2009) including Nevado Ampato in the Cordillera Chila (Úbeda et al., 2009; Alcalá et al., 2010).

Ice cores provide a range of geochemical and biological proxies including pollen grains, which can be used for paleoclimate reconstructions (e.g. Thompson et al., 2000; Liu et al., 2007; Kellerhals et al., 2010; Reese et al., 2013). However, oxygen isotope values ($\delta^{18}O$) in ice cores, which is used as a proxy for temperature in high latitudes, is primarily influenced by precipitation and ENSO event frequency in the Central Andes (e.g. Hoffmann et al., 2003; Vimeux et al., 2005). The nearest ice record to the study area (100 km to W) was recovered from the summit of Nevado Coropuna. The core contains ice layers from the last 20 ka but it is still being analysed (Vimeux et al., 2009). The only analysed ice core which represents the semi-arid Western Cordillera was drilled on Nevado Sajama about 400 km to SSE from the study area. The record covers the last 25 ka with seasonal to decadal resolution over the last 1000 years (Thompson et al., 1998).

1.2. Holocene climate changes

The climate conditions in the Western Cordillera during the Early Holocene (~12–8 ka *sensu* Walker et al., 2012) are poorly defined and available studies provide only fragmented paleoclimate information for this period. The thermal gradient of SST between the eastern and western tropical Pacific was lower by ~1 °C than today, the mean position of the ITCZ was located farther north (Martin et al., 1997) and the intensity of the Bolivian High was reduced (Silva Dias et al., 2009). Weak ENSO conditions with La Niña-like pattern prevailed and the Western Cordillera probably experienced increased precipitation (Placzek et al., 2001; Carré

et al., 2012). Between ~12.5 and 10 cal. ka BP temperatures were 3–5 °C lower than today based on pollen analyses (Graf, 1994) and climate-glacier modelling (Kull and Grosjean, 2000). After ~10 cal. ka BP a significant warming occurred and the temperature gradually increased to the highest postglacial values (Baied and Wheeler, 1993; Bush et al., 2005). In the northern segment of the Western Cordillera, warm conditions culminated ~8.5 cal. ka BP when the temperatures were ~1.5–2.0 °C warmer than today (Thompson et al., 2006; Weng et al., 2006). Overall, the Early Holocene was warmer than the Middle to Late Holocene, based on pollen data (Hansen et al., 1984, 1994; Markgraf, 1989), treeline position (Bush et al., 2004, 2005) and *Distichia muscoides* deposits (Thompson et al., 2006; Buffen et al., 2009).

During the Middle Holocene (~8–4 ka), the ITCZ started to advance southward and the magnitude and frequency of El Niño events have gradually increased (Clement et al., 2000; Koutavas and Lynch-Stieglitz, 2004). The $\delta^{18}O$ values of fish otoliths from the Peruvian coast indicate 3–4 °C warmer SSTs prior to 6 ka BP than today (Andrus et al., 2002). The climate in the Western Cordillera seems to remain relatively wet and warm until ~5.2–5.0 cal. ka BP (Thompson et al., 1998; Kuentz et al., 2012) when a prominent shift in the ITCZ position occurred and a period of stronger ENSO activity started (Fig. 2; Rodbell et al., 1999). These changes probably forced the strong westerlies that inhibited moisture advection from the east leading to the preliminary drier and colder conditions at the end of the Middle Holocene (Thompson et al., 1995; Schittek et al., 2014) and in the Late Holocene (Weng et al., 2004; Thompson et al., 2006). An opposite trend has been reported from the Altiplano and Eastern Andes where proxy records from ice cores, lake sediments, speleothems and wetlands indicate dry interval with episodic wet events between ~8 and 5 ka and subsequent increase in the intensity of convection associated with the SASM in the Late Holocene (e.g. Valencia et al., 2010; Bird et al., 2011a; Ledru et al., 2013).

Since the beginning of the Late Holocene the summer insolation increased and around 3 ka BP it was high enough to produce strong upper troposphere easterlies that initiated a summer precipitation regime in the Western Cordillera (Baker et al., 2001; Kuentz et al., 2012). The climate change led to glacier advances as indicated by moraine ages of 3.3–1.7 ka BP in the Cordillera Blanca, Cordillera Raura and Sajama (Clapperton, 1983; Rodbell, 1992; Smith et al., 2009). The return of more humid conditions matches the timing of a global climate change around 2.8 cal. ka BP (Van Geel et al., 1996; Chambers et al., 2007) that, however, has not been recognized in proxies from the Western Cordillera yet. The summer precipitation regime was accompanied by warming until ~1 cal. ka BP, when a prominent dry and cold episode occurred (Kuentz et al., 2012). The dry conditions correspond with the weakened SASM that is indicated by higher $\delta^{18}O$ in lake sediments and speleothems in the Eastern Cordillera (Fig. 2; Bird et al., 2011a; Kanner et al., 2013). The climate in the Western Cordillera sustained predominantly dry to the end of the 16th century, when it returned to wetter conditions as indicated by the Little Ice Age (LIA) moraines (Solomina et al., 2007; Jomelli et al., 2009) and tree-rings (Morales et al., 2012). The temperature during the LIA interval (AD 1520–1880; Thompson et al., 2013) decreased significantly being as much as ~0.7 °C colder in the Ampato volcanic complex than at present (Alcalá et al., 2010). The last prominent decrease in precipitation occurred in the mid-18th to late 19th centuries enhancing a retreat of glaciers (Liu et al., 2005; Jomelli et al., 2009). The return to dry conditions is consistent with reduced SASM precipitation in the Eastern Cordillera that is recorded as an abrupt increase in $\delta^{18}O$ records (Fig. 2; Bird et al., 2011a). A significant warming occurred in the 20th century as indicated by instrumental temperature records (Vuille and Bradley, 2000). The analysis of air temperature in modern weather records reveals a warming trend of 0.10 °C/decade and an overall temperature increase of 0.68 °C between 1939 and 2006 (Vuille et al., 2008). A general tendency toward slightly drier conditions was reported in southern Peru for the second half of the 20th century (Vuille et al., 2003) although neither a trend nor mean change in rainfall was observed (Lavado Casimiro et al., 2013).

2. Regional setting

The study area is situated near Nevado Mismi in the Cordillera Chila, which is a part of the Western Cordillera of the Central Andes in southern Peru (Fig. 1). The sampling sites are located in the Carhuasanta valley on the Atlantic side of the main continental divide (Fig. 3). The upper reaches of the valley are cut into the divide range, which consists of andesitic lavas (Davila, 1988). The middle section of the Carhuasanta valley is built mainly of pyroclastics, whereas the lower part of this valley down to the confluence with the Apacheta River consists of rhyolitic lavas. The preserved volcanic formations originated in the Neogene except for andesitic lavas, which formed around 2.35 Ma (Lajo and Nuñez Juarez, 2008). The recent deposition of volcanic material is limited to ash-fall from the nearest active volcanoes (e.g. Juvigné et al., 2008) located 35 km to the SW (Sabancaya), 60 km to the W (Andahua) and more than 90 km to the SE (Misti, Ubinas).

The Carhuasanta valley was transformed by glaciers and its lower part has the form of a trough. The wide and slightly inclined trough floor is filled with peat accumulations of *Distichia muscoides* (Juncaceae), which forms layers of humolites several metres thick (Engel, 2002). Relatively diverse wetland vegetation covers the peat bogs, where seasonal grazing of alpacas and llamas takes place. The vegetation is dominated by cushion plants or dwarf shrubs, e.g. *Aciachne pulvinata*, *Pycnophyllum mole*, *Plantago sp.*, *Carex sp.* and *Juncus* sp. (Šefrna et al., 2008). Above the peat bogs, occasional scattered grasses, dwarf shrubs, cushion and succulent plants occur. The sparse vegetation reflects perennial frosts and low precipitation, forming a characteristic dry puna ecosystem. The grasses are predominantly represented by genera *Calamagrostis*, *Agrostis*, *Festuca* and *Stipa*, shrubs are dominated by tola formation (*Lepidophyllum quadrangulare*, *Chuquiragua sp.*, *Baccharis sp.*) and the cushion plants by *Alchemila diplophylla*, *Azorella compacta*, *Xenophyllum lycopodioides*, *Chevreulia sp.* and *Senecio* sp. (Šefrna et al., 2008).

The climate is characterized by the mean annual air temperature around 0 °C and precipitation up to 800 mm/year (Skrzypek et al., 2011). The temperature varies slightly between the seasons, but diurnal variations in the troughs exceed 30 °C during dry austral winters. The number of frost days increases with altitude to more than 300 days/year at 5150 m a.s.l. (Skrzypek et al., 2011). Precipitation occurs during austral summers that contribute more than ~60% of the total annual precipitation. Long-lasting and continuous precipitation occurs between December and March, when the monsoonal precipitation shifts southward from Amazonia (Falvey and Garreaud, 2005). Snow cover forms sporadically in winter and usually only lasts for a few hours.

Due to the location of the Carhuasanta valley in the high mountain area, it is little influenced by anthropogenic disturbances. The only human activity in the valley is grazing that probably dates back to pre-Columbian times when an important route from the Colca valley over the continental divide was established (Treacy, 1994). Regarding that camelids were grazed within the high puna prior to a period of human expansion, an anthropogenic enhancement of grazing probably has little effect on the vegetation or hydrology of the peatbog ecosystem. Mining in the nearby Apurímac and Colca valleys probably started in pre-Columbian times and it

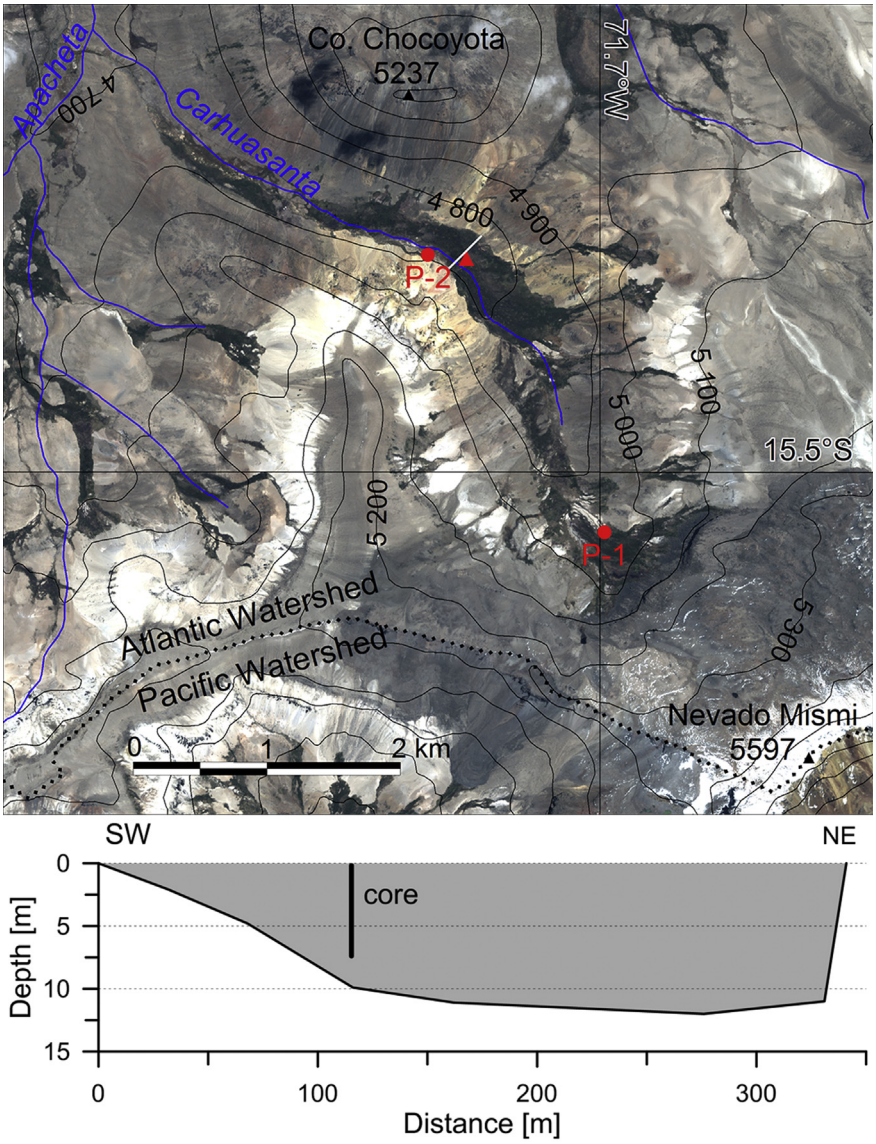

Fig. 3. Location of the core (red triangle) and dated peat profiles P-1 and P-2 (red circles) in the Carhuasanta valley. White line indicates the location of the depth profile shown at the bottom. (For interpretation of the references to colour in this figure legend, the reader is referred to the web version of this article.)

was the most intensive in the 17th and 18th centuries (Paulo and Gałaś, 2008). Silver extraction flourished in Caylloma and other mining districts around the study area, including Arcata, Orcopampa and Madrigal (Fig. 1). The main ores included Ag and Au during the colonial mining but polymetalic veins started to be exploited in the 20th century (Candiotti de Los Rios et al., 1990). Ore minerals include Pb, Ag sulfosalts with high contents of Cu, As, Sb and Fe (Echavarria et al., 2006).

3. Material and methods

The organic matter analysed in this study comes from the largest in-situ accumulated peat-bog in the central part of the Carhuasanta valley. The depth of the bog was measured along a longitudinal transect and two cross-sections using a gauge auger. On the basis of the measurement, the deposit thickness map was constructed and a position of the core was selected (Fig. 3). The core site (15°29′6″S, 71°42′34″W, 4809 m a.s.l.) was located about 150 m to the NE of the southern border of the bog (Figs. 4 and 5A). The core was drilled close to the valley axis where more than 10 m deep accumulation of peat was measured. The present vegetation is dominated by *Distichia muscoides* that is well adapted to diurnal freezing and thawing in wetlands (Squeo et al., 2006; Thompson et al., 2006). The *Distichia* remains are very well preserved in the bog due to the waterlogged conditions and low ground temperatures for a big part of the year. The measurements of ground temperature profile down to the 150 cm depth in 4890 and 4985 m a.s.l. revealed that the temperature ranges from 1 to 4 °C. The temperature measurements were made in 2007–2008 using thermistors with the accuracy of ±0.2 °C connected to Minikin (EMS Brno/Czech Republic) data loggers. A 755-cm-long core was sampled using the Eijkelkamp peat sampler, collected as uncompressed cores in 50-cm-long sections. The upper 20 cm of the core contained relatively fresh plant material and was sampled with a shovel. The colour of sediments was classified with the Munsell Soil Color Chart (2000). The whole core was divided into 2.5-cm slices. *Distichia* remains form peat slices were homogenized and dried for a stable isotope analysis (0.1 g sample powder), metal content, and lead (Pb) isotopic

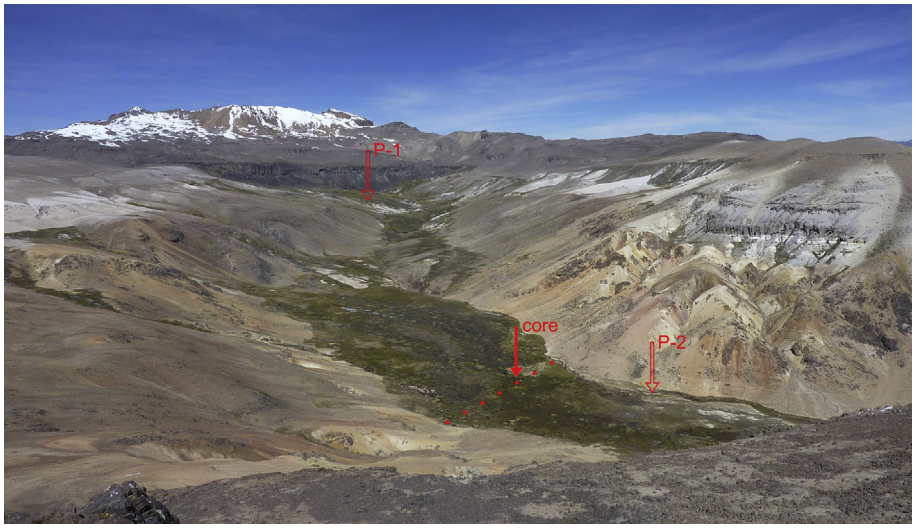

Fig. 4. The Carhuasanta valley with locations of the core site and the peat profiles P-1 and P-2 as seen from the north towards Nevado Mismi during the dry winter season (July 2011). Red dots mark the position of a cross-profile where depth of the bog was probed. (For interpretation of the references to colour in this figure legend, the reader is referred to the web version of this article.)

analyses (0.5 g). Single macroremains of *Distichia* peat were also extracted from 14 slices (from 25 cm to 735 cm depth) for radiocarbon dating. In order to obtain better control of the *Distichia* peat growth rate, peat profiles P-1 and P-2 were additionally sampled for the dating in different geomorphological positions within the valley (Figs. 3 and 5BC).

The core samples were analysed for stable nitrogen and carbon isotope compositions ($\delta^{15}N$ and $\delta^{13}C$), using a continuous flow system consisting of the Delta V Plus mass spectrometer connected with the elemental analyser Thermo Flush 1112 via Conflo IV (Thermo-Finnigan/Germany) in West Australian Biogeochemistry Centre, The University of Western Australia. In the elemental analyser, the samples were oxidized quantitatively (Pella, 1990; Skrzypek and Paul, 2006) and yielded N_2 and CO_2 gases were introduced in a stream of helium into the Isotope Ratio Mass Spectrometer (IRMS) as transient peaks. Stable nitrogen and carbon

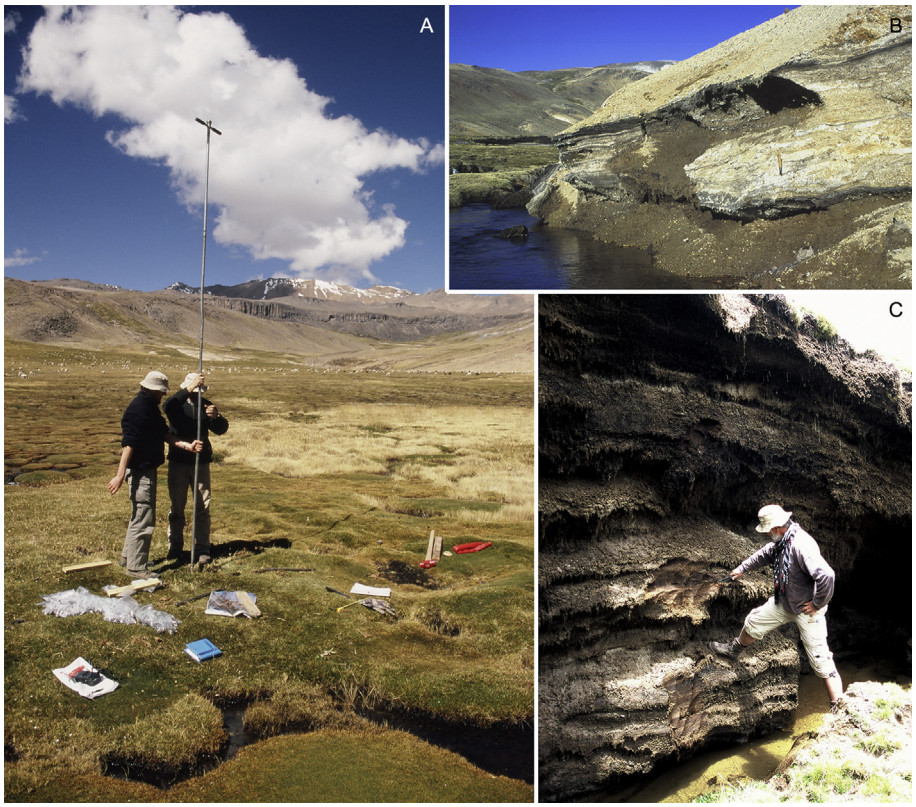

Fig. 5. Study sites in the Carhuasanta valley. A – the core site; B – the debris-covered peat profile P-2; C – the dissected peat profile P-1.

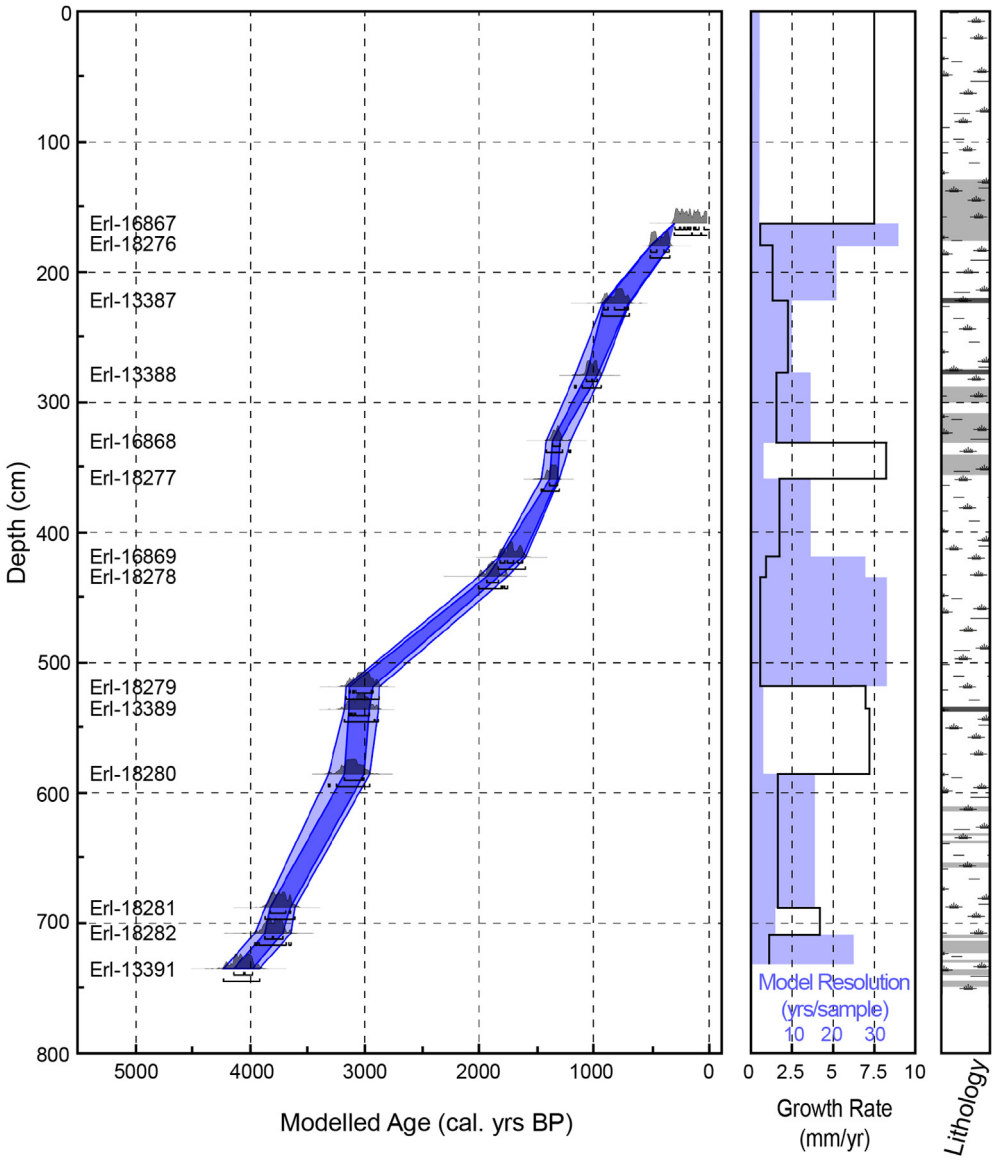

Fig. 6. Age–depth model, growth rate and lithology of the Carhuasanta peat core. Probability distributions for the single calibrated dates are shown in grey, whereas the depth model curves represent envelopes for the 95% and 68% probability density ranges. Details of ^{14}C dates are given in Table 2. Lithology panel shows dark and light brown silty layers (dark and light shading) in the peat core.

isotope compositions were reported as the standard δ-notation (e.g. Skrzypek, 2013) in permil after the multi-point normalization of raw data to the isotope international scale directly using the international standards provided by International Atomic Energy Agency ($\delta^{13}C$ – NBS22, USGS24, NBS19, LSVEC; $\delta^{15}N$ – N1, N2, N3) and the laboratory standards following selection as by Skrzypek et al. (2010) and values as in Skrzypek (2013). The uncertainty associated with the stable isotope analyses (1σ standard deviation) was not more than 0.10‰.

Pb isotopic ratios ($^{206}Pb/^{207}Pb$ and $^{208}Pb/^{206}Pb$) and concentrations of Al, As, Ca, Mg, Pb, Rb, Sc and Ti were measured in core samples and main rocks in the valley. Peat samples (0.5 g) were ashed with a temperature increase of 1 °C min^{-1} to the maximum temperature of 450 °C. The total mineralization time was 10 h. The sample was subsequently dampened with deionized water and dissolved in 5 ml of HF (49% v/v) and 0.5 ml of $HClO_4$ (70% v/v). The mixture of acids was evaporated on a hot plate (150 °C) to near dryness and this step was repeated once. The residue was dissolved in 2 ml of concentrated HNO_3, filled to 100 ml with DIW and transferred to a 100 ml HDPE bottle. Rock samples (0.1 g, pulverized down to 200 mesh) were digested in 10 ml HF and 1 ml $HClO_4$ overnight on a hot plate (150 °C) and evaporated to 0.5 ml of the digest, which was dissolved in 2% (v/v) HNO_3 and transferred to a 100 ml flask. The concentration of elements was determined (e.g. Strnad et al., 2009) by inductively coupled plasma quadrupole based mass spectrometry (ICP MS, X Series 2, Thermo Scientific). The quality of the measured data was validated using measurements of the reference materials SRM 1575 (Pine needles, NIST, USA) and rock samples BCR 2 and AGV 2 certified by the US Geological Survey (USGS, 1998).The differences in the measured and certified values did not exceed 3% RSD. The concentration of the elements was standardized using Z scores and the relationships between elements were visualized by the principal component analysis using Canoco 4.55 software (ter Braak and Šmilauer, 2002).

Environmental magnetic susceptibility was measured in discrete samples from mineral-rich core sections and compared

Table 2
Radiocarbon dates and calibrated ages for peat profiles in the Carhuasanta valley. Calibrated age based on the median of the probability distribution is reported in cal. yrs BP and BC/AD years. Calibration with OxCal 4.2.3 (Bronk Ramsey, 2009) using SHCal13 (Hogg et al., 2013).

Site	Depth [cm]	Laboratory code	Radiocarbon age [^{14}C yrs BP]	Calibrated age		Growth rate [mm yr^{-1}]
				[cal. yrs BP]	[BC/AD]	
Core	160	Erl-16867	184 ± 45	155 ± 86	1796	7.5
	177.5	Erl-18276	401 ± 39	410 ± 55	1541	0.7
	222	Erl-13387	909 ± 68	782 ± 69	1168	1.2
	277.5	Erl-13388	1148 ± 44	1009 ± 48	941	2.4
	327.5	Erl-16868	1454 ± 47	1317 ± 40	633	1.6
	357.5	Erl-18277	1512 ± 42	1354 ± 40	597	8.1
	417.5	Erl-16869	1831 ± 47	1713 ± 68	237	1.7
	432.5	Erl-18278	1972 ± 43	1880 ± 59	71	0.9
	517.5	Erl-18279	2927 ± 47	3016 ± 78	−1067	0.7
	535	Erl-13389	2945 ± 45	3040 ± 76	−1091	7.3
	585	Erl-18280	2994 ± 45	3108 ± 79	−1159	7.4
	687.5	Erl-18281	3516 ± 46	3748 ± 68	−1799	1.6
	707.5	Erl-18282	3570 ± 46	3799 ± 73	−1850	3.9
	735	Erl-13391	3771 ± 47	4078 ± 81	−2129	1.0
P-1	440	Erl-11280	1509 ± 58	1360 ± 56	590	3.2
P-2	110	CU-1650	1565 ± 174	1444 ± 187	507	0.8

with magnetic properties of pure peat samples from 380 cm to 590 cm depth. Magnetic susceptibility measurements were made using the SM-30 m (ZH instruments/Czech Republic).

14 selected samples from the core and one sample from the lowermost section of the peat profile P-1 were dated using the accelerator mass spectrometry (AMS) at the Radiocarbon Laboratory of Erlangen, the University of Erlangen, Germany. The samples were prepared with the acid-alkali-acid method, using HCl and NaOH, and centrifuged with a $ZnCl_2$ solution. In addition, a sample of basal peat from the profile P-2 was dated using liquid scintillation counting at the Radiocarbon Laboratory of Charles University in Prague, Czech Republic. Conventional ^{14}C ages of samples were calibrated using OxCal 4.2 software (Bronk Ramsey, 2009) and SHCal13 (Hogg et al., 2013). All radiocarbon dates are reported as calibrated years before present (cal. yrs BP).

4. Results

4.1. Core description

The *Distichia* peat dominates the whole 755-cm-long core except for three short sections with the increased content of fine (sandy silt) mineral material. Typically, the growth of *Distichia muscoides* restricts other plants occurrence due to more effective morphological and physiological adaptations (Balslev, 1996; van der Hammen and Santos, 2003), therefore the *Distichia* remains constitute ~99% of the organic matter in the core. The upper part of the core from the surface to the depth of 128 cm is mainly composed of very well preserved rootlets and vegetative remains of *Distichia muscoides*. This section has an ochre colour, which continuously changes downwards to a lighter shade (from 2.5Y 6/4 to 2.5Y 5/3). The carbon content varies between 36.6 and 48.7%. The colour of the samples becomes brown (2.5Y 4/4) down to 176 cm. The samples between 128 and 176 cm have a generally high proportion of mineral material and a low proportion of organic carbon (11.6–25.0%) compared to the samples from the upper part of this section of the profile.

Between 176 cm and 288 cm, the dark brown (2.5Y 4/3) decomposed peat prevails with two thin darker layers (2.5Y 3/2) at 220.5–222 cm and 275–277 cm (Fig. 6). In the organic-rich lighter sections the carbon content ranges mostly from 32 to 53% whereas in the upper and lower intercalated dark layers it varies between 27% and 23%. The second section of predominantly mineral material with brown colour (2.5Y 5/4) can be found between 288 cm and 355 cm. The carbon content is generally low (28.8–13.7%) except for two interleaved sections of decomposed peat at 300–309 cm and 332–339 cm (31.0–40.4%). The sediment between 355 cm and 709 cm is dominated by dark brown (2.5Y 4/4) decomposed peat with carbon content values between 17.5 and 49.4%. Within this section, apparently darker (2.5Y 3/2) matter with carbon content ~35% can be found at 534–537 cm and four thin layers with a generally low proportion of carbon (16.0–28.5%) occur at 610–613, 633–634, 637–638 and 653–657 cm. The lowermost cored section below 709 cm is characterized by darker (2.5Y 4/3) mineral-rich layers (709–712, 715–723, 728–730, 736–740 and 744–748 cm) and interleaved decomposed peat sequences with a lighter colour (2.5Y 5/4). The carbon contents in the predominantly mineral and decomposed peat layers range from 17.3 to 27.7% and from 28.2 to 35.9%, respectively. However, *Distichia* remains dominate organic matter in the whole core including the "mineral-rich" sections with low C%.

4.2. Age–depth model

The radiocarbon data of the analysed samples are consistent within the core, decreasing from the lowermost core section towards the surface (Table 2). The mean age of 4078 ± 81 cal. yrs BP obtained for the organic matter at the depth of 735 cm indicates that the cored samples deposited during the last ~4.3 cal. ka BP, i.e. mostly within the Late Holocene *sensu* Walker et al. (2012). The mean age of 155 ± 86 cal. yrs BP was obtained for the sediment sampled at the depth of 160 cm. The correlation between the calibrated age and the depth of the 14 samples from the section between 160 cm and 735 cm was adopted for the age determination of core sections between two successive radiocarbon dates. The linear regression equation ($y = 0.1451x + 133.68$; $R^2 = 0.98$, $p < 0.001$) was also used for the calculation of the rate of *Distichia* peat accumulation within the core. The mean accumulation rate ranges from 0.7 to 8.1 mm yr^{-1} in the sections between the dated sample pairs in the core (Table 2 and Fig. 6). The variation in the accumulation rate is generally small (1–4 mm yr^{-1}), suggesting steady accumulation of the *Distichia* peat for most of the last ~4.3 ka. A significantly higher mean rate of accumulation (7–8 mm yr^{-1}) was calculated for the three core sections in the depth of 585–517.5, 357.5–327.5 and 160–0 cm. The range of values calculated for the rate of peat accumulation within the core is in agreement with the mean rate of accumulation in the peat profiles P-1 and P-2 (Table 2). The rate of 3.2 mm yr^{-1} was calculated for the P-1 profile in the central part of the peat bog. The value of 0.8 mm yr^{-1} represents the rate of *Distichia* peat accumulation within the south-western margin of the peat bog, where the growth of the peat is occasionally disturbed by input of colluvial deposits from the adjacent valley slope (Fig. 5B).

4.3. Variation in $\delta^{13}C$ and $\delta^{15}N$ values

The stable carbon and nitrogen isotope compositions of *Distichia* remains preserved in the peat core were analysed in 302 samples (Fig. 7). $\delta^{13}C$ and $\delta^{15}N$ vary in the range expected for C3 type plants (e.g. Skrzypek et al., 2010). The highest $\delta^{13}C$ value in the core was −23.62‰ (depth 517.5 cm) while the lowest $\delta^{13}C$ value was −28.45‰ (depth 530 cm). Hence, the maximum range of the $\delta^{13}C$ variation in the core embraces 4.83‰, with the mean for the core −26.25 ± 0.65‰ (±one standard variation). The $\delta^{15}N$ values vary between 2.99‰ and −2.05‰, with the mean value 0.53 ± 0.97‰. In the studied core, both $\delta^{13}C$ and $\delta^{15}N$ varied with the depth over the last four millennia. However, the changes in $\delta^{13}C$

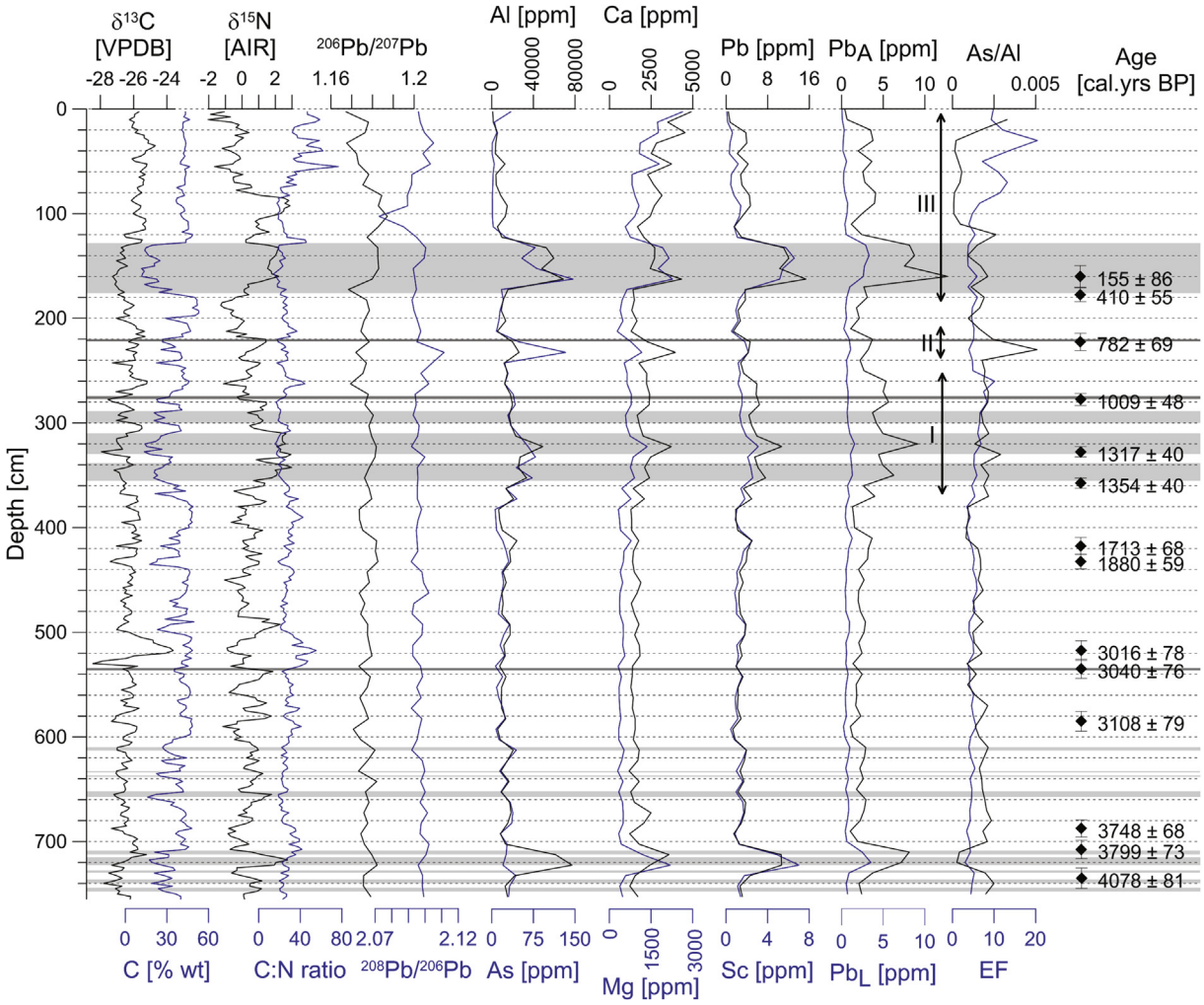

Fig. 7. Stable carbon and nitrogen isotope compositions, C%, N% and selected metal concentrations in the Carhuasanta core. Lithogenic (Pb_L) and anthropogenic lead (Pb_A), enrichment factor (EF) and arsenic normalized to aluminium in the core. Collaque (I), Inca (II) and Colonial (III) periods of anthropogenic enrichment resulting from regional mining and smelting in the Colca valley (after Treacy, 1994) are indicated with black lines. Grey panels indicate sections with higher mineral content and black diamonds with error bars show calibrated ages and uncertainty of our chronological data.

and $\delta^{15}N$ are not contaminant. The highest range of progressive changes in $\delta^{13}C$ in the whole was observed in a relatively short section of the core (517.5–530 cm), which reflects the time span between 3020 and 3030 cal. yrs BP. Over just two decades $\delta^{13}C$ increased by 4.83‰, which is also the maximum range of $\delta^{13}C$ values observed in the core. The second highest range of subsequent changes is recorded in the adjacent section (500–517.5 cm) in which a significant decrease from −23.62‰ (depth 517.5 cm, 3020 cal. yrs BP) to −26.27‰ (depth 500 cm, 2780 cal. yrs BP) was observed. The range of the variations in the remaining part or the core (excluding 500–530 cm section) is much lower and equals 3.25‰, $\delta^{13}C$ between −24.69 and −27.94‰.

4.4. Variation in metal concentrations, lead isotope ratios and magnetic susceptibility

The concentrations of the metal elements show a similar pattern within the core increasing significantly in the mineral-rich sections (Fig. 7). In the upper one metre of the core, the concentrations are below background core levels and most elements show a decreasing trend except for biogenic elements Ca and Mg, which increase. Below this section, the element concentrations increase by an order of magnitude in the three mineral-rich sections culminating in the depth of 130–180 cm (~120–430 cal. yrs BP), 320–350 cm (1270–1350 cal. yrs BP) and 710–720 cm (3820–3930 cal. yrs BP). The highest concentration levels are recorded between 710 and 720 cm (3820–3930 cal. yrs BP) where concentrations increase by an order of magnitude above background by an order of magnitude values for most of the elements (except As and Ca). The patterns of C and N concentrations are inversely related to element concentrations (Fig. 8). Therefore, higher metal concentrations are observed in the sections with higher mineral concentrations, reflecting metal concentrations in source rocks for inorganic sediments.

The concentration level of Pb shows the most prominent peak at 160 cm and two minor peaks at the depth of 320 cm and 710–720 cm. The values obtained for Pb isotope ratios range from 1.167 to 1.187 ($^{206}Pb/^{207}Pb$) and 2.072 to 2.111 ($^{208}Pb/^{206}Pb$). The isotope ratios show a similar pattern within the core with minor differences below 280 cm depth and more pronounced variations in the upper part of the profile. The isotope ratios $^{206}Pb/^{207}Pb$ and $^{208}Pb/^{206}Pb$ obtained for the section above 100 cm show a gradually decreasing/increasing trend. Fig. 9 shows the magnetic susceptibility within the core. The magnetic susceptibility in the samples

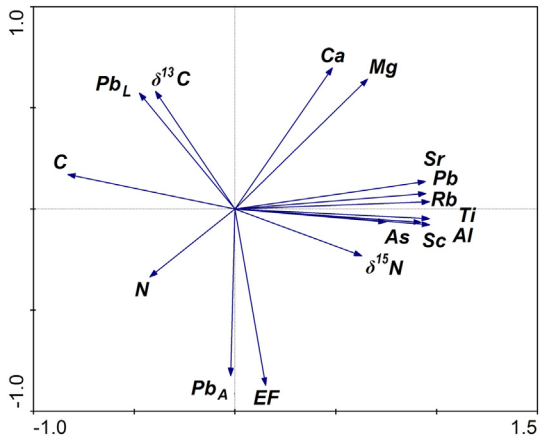

Fig. 8. PCA ordination of element concentrations in the core. The first two axes explaining 64.5% of variability are shown.

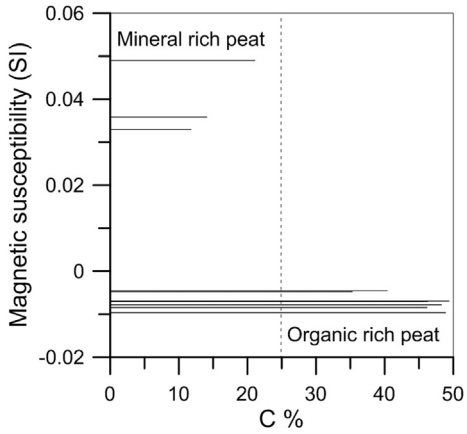

Fig. 9. Difference in magnetic susceptibility of mineral-rich and organic-rich *Distichia* peat.

from the mineral-rich core sections is varying from 0.03 to 0.05 SI. These values differ significantly from the background levels in the pure peat that are lower than −0.005 SI.

5. Discussion

5.1. Distichia peat as a record of paleoclimate changes

The $\delta^{13}C$ value of living *Distichia* plants from the area of the core collection varied in the range of 2.6‰, from −26.9‰ at 4356 m a.s.l. to −24.3‰ at 5049 m a.s.l., and showed a strong relationship with the altitude of the plant sampling location (Skrzypek et al., 2011). Consequently, the highest $\delta^{13}C$ values were characteristic of the highest altitudes. This observed altitudinal trend in $\delta^{13}C$ is in agreement with other studies based on lower plants from Europe (e.g. Skrzypek et al., 2007). A similar relationship to that seen for plants was also observed for peat samples collected from various altitudes in Europe (Skrzypek et al., 2010) and at our study site (Skrzypek et al., 2011). Several authors have investigated the meaning of the $\delta^{13}C$ value in peat and peat-forming plants, especially in the *Sphagnum* genera (including Ménot-Combes et al., 2004; Loader et al., 2007; Moschen et al., 2009; Brader et al., 2010; Tillman et al., 2010; Skrzypek et al., 2013) and have considered environmental factors such as air temperature, humidity, precipitation, vapour pressure deficit and atmospheric CO_2 concentration. Despite the possibility of a combined influence of a few factors, the air temperature of the growth season seems to be the major factor governing $\delta^{13}C$ of *Distichia* macrofossils well preserved in peat sediments (Skrzypek et al., 2011). Our initial calibration, based on an altitudinal transect that intersects the core collection site, indicated that the observed decrease of ~0.97 ± 0.23‰ in the stable carbon isotope composition of *Distichia* peat reflects a 1 °C increase in the mean air temperature of the growing seasons at the ground level. The temperature at the ground level at high altitudes largely reflects insolation. In contrast, no obvious relationship was observed between precipitation and the stable carbon isotope composition of *Distichia* peat (Skrzypek et al., 2011).

We built on this previous calibration and reconstructed temperature variations of the growing (warmest) season (September to November) over the last four millennia for the Central Andes. These reconstructions were compared with other available paleoclimate reconstructions for this region. This comparison allowed cross-verification of our new peat proxy with other independent proxies. The proposed reconstruction was based on the assumption that *Distichia* plant macrofossils were well-preserved in peat and that, after the initial partial decomposition of fresh plant material, the original relative differences in plant $\delta^{13}C$ remained preserved in the peat. The observed high preservation of *Distichia* macrofossils in peat likely resulted from the high water table, acidic conditions (pH 5–6) and stable very low temperature in the sediment (1–4 °C as measured at various depths in several locations in the valley). Very good preservation was also confirmed by the low values and low variations in C/N ratio in the core, which ranged from 15 to 40 for 91% of samples (mean 26.2 ± 5.6). The variations in C% and N%, as well as $\delta^{13}C$ and $\delta^{15}N$, in plants are not directly linked due to different metabolic pathways for acquisition of these two elements by the plants (CO_2 from the atmosphere and NO_3 or NH_4 from water). On the other hand, $\delta^{13}C$, $\delta^{15}N$ and C% and N% can be correlated if organic matter is significantly decomposed, as ^{13}C and ^{15}N usually undergo preferential removal during biological decomposition (Engel et al., 2010). This is not the case in the studied core, as confirmed by a principal component analysis (PCA), which shows that both N and C variations are driven by different independent factors (Fig. 8). However, few sections with high mineral contents can be considered more decomposed as a result of the drier conditions and consequent decrease in the water table level (von Post, 1946).

The carbon and nitrogen percentages themselves are not indicative of the stage of decomposition, as they varied along with the variations in addition of inorganic material deposited in the peat (Engel et al., 2010). The lower C% reflects a higher addition of the mineral contents, such as clay, silt or fine sand (Fig. 7). Therefore, the lower C% reflects an increased volcanic ash deposition or higher erosion in the upper part of the catchment due to the higher outflows and seasonal waterlogging of the peat bog. The very low temperature, resulting from the high altitude of the sampling point, means that almost all of the precipitation occurs as snow or hail. Therefore, the higher outflow indicates not only the higher annual precipitation but also warmer conditions, which allowed rapid thawing of freshly fallen snow and greater outflow from perennial snow fields (Janský et al., 2011).

In the studied location, lower $\delta^{13}C$ values, indicative of higher temperatures, are usually associated with lower C%, indicative of higher outflow and bog waterlogging. This pattern in $\delta^{13}C$–C% relation shows stronger and significant correlations for the core sections with low and variable C%, such as in the mineral-rich core sections (e.g. 205–370 cm, 640–1430 cal. yrs BP, $R^2 = 0.61$, $p < 0.001$, C = 32.5 ± 9.1%) in contrast to the organic-rich sections with less variable C% (e.g. 440–600 cm, 1980–3200 cal. yrs BP,

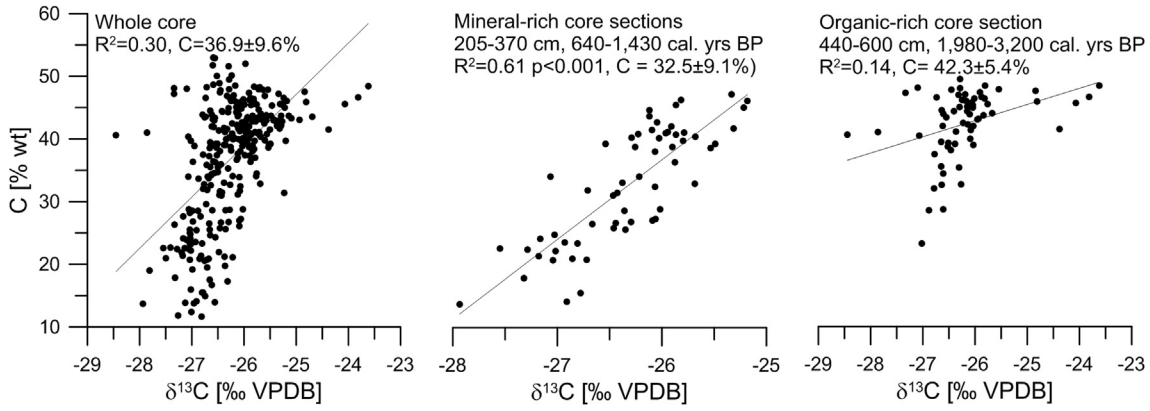

Fig. 10. Correlation between $\delta^{13}C$ and C% of organic matter in the core in relation to admixture of inorganic material deposited on the bog surface.

R^2 = 0.14, C = 42.3 ± 5.4%) and the whole core (R^2 = 0.30, C = 36.9 ± 9.6%) (Fig. 10). Following this reasoning, the drier and colder conditions at the studied location resulted in more positive $\delta^{13}C$ values and in higher C%, as less inorganic material will be deposited on the bog surface due to lower run off. The link between the amount of precipitation and temperature can be attributed to the mean annual cycle of the atmospheric circulation. The area remains dry for most of the year due to dominant westerly air flow. The extremely dry period coincides with the coldest months around the summer solstice (May–August). Intense ground surface heating in austral spring and summer destabilizes the troposphere above the Altiplano and establishes an upper-level easterly circulation with strong convective storms that bring the most significant annual precipitation (Garreaud et al., 2003). The interannual variability of the temperature and precipitation is dominated by ENSO impacts although the linkage mechanism remains poorly understood. There is an opposite tendency, towards drier and warmer conditions, during El Niño years but the precipitation is only weakly related to the ENSO indices (Lagos et al., 2008; Garreaud et al., 2009).

5.2. Origin of mineral material in the core

The decrease in $\delta^{13}C$ and C% observed in the mineral-rich core sections is associated with significantly higher concentrations of metal elements. The metal concentrations reflect the changes in the rate of erosion and/or accumulation on the bog surface and may be used as an indicator of either natural or anthropogenic increase in metal concentration in the sediment. In order to distinguish the source of the mineral material in the core, concentrations of natural and anthropogenic Pb (Fig. 7) were determined using scandium as the reference element (Shotyk et al., 2000). Anthropogenic Pb dominates the core showing major peaks in all three mineral-rich sections. The concentration level of this element increases in the upper part of the core culminating in the sections 130–180 cm (120–430 cal. yrs BP) and 320–350 cm (1270–1350 cal. yrs BP). The concentration of lithogenic Pb increases significantly between 160 and 130 cm (160–120 cal. yrs BP) and between 740 and 720 cm (4130–3930 cal. yrs BP). The variations in anthropogenic and lithogenic Pb suggest that the observed rise in the metal deposition after 1350 cal. yrs BP is associated with the regional metallurgical activity whereas the enrichment event around 4 cal. ka BP may be also attributed to natural sources.

The anthropogenic enrichment of the upper two mineral-rich sections is also indicated by significantly higher concentrations of arsenic, which is abundant in local ores (Echavarria et al., 2006). The most significant increase in As concentration occurs in the depth of 160 cm (155 cal. yrs BP) and 230 cm (810 cal. yrs BP) where it exceeds 130 ppm, more than order of magnitude above the background level. A minor increase in As concentration is recorded between 370 and 330 cm (1430–1320 cal. yrs BP), which is the oldest section of the core with As enrichment. Based on the radiocarbon dating the youngest rise in the metal content could be connected with Colonial mining and smelting in the 16th to 19th centuries (Chapman and Kelly, 2013) and the previous enrichments with the Inca metallurgical activities during the Late Intermediate Period (850–500 cal. yrs BP; AD 1100–1450) and Collaque (Wari) Empire (1350–850 cal. yrs BP; AD 600–1100) (Treacy, 1994).

Stable isotope ratios obtained for Pb allow for confirmation of different sources of Pb within the core. The isotope values recorded at the depth of 710–720 cm (3930–3830 cal. yrs BP) range up to about 1.182 ($^{206}Pb/^{207}Pb$) and 2.101 ($^{208}Pb/^{206}Pb$). By contrast, the isotopic values obtained for the depth of 170 cm are 1.168 ($^{206}Pb/^{207}Pb$) and 2.095 ($^{208}Pb/^{206}Pb$). Higher variations in the Pb ratios in the upper part of the core could be explained by contamination associated with the mining and smelting activities around the study area. The source of contamination in the upper 30-cm core section (since the late 1960ies) may be attributed to petroleum products combustion (e.g. gasoline or fuel oils). Pb isotope values at the depth of 710–720 cm vary around the background level for the core implying environmental conditions without any anthropogenic influence. The natural origin of this section is also indicated by significantly higher magnetic susceptibility of the sediment, which belongs to the most characteristic indicators of volcanic ash (Gonzalez et al., 1999). The increase in Pb isotope values, lithogenic Pb and metal elements concentrations in the core occurs around 4078 ± 81 cal. yrs BP (Fig. 7) correlating with tephra eruption of El Misti volcano dated 4102 ± 89 cal. yrs BP (3800 ± 50 yrs BP; Thouret et al., 2001).

5.3. Paleoclimate over the last 4300 years

We used $\delta^{13}C$ and C% of *Distichia* peat as temperature proxies to reconstruct the paleoclimate over ~4300 years of peat deposition in the Carhuasanta valley. Following the above discussion, a lower $\delta^{13}C$ value indicates a higher temperature during the growth season, while a lower C% indicates wetter conditions, likely due to a warmer austral summer and higher runoff from the upper part of the catchment. The relative mean change in the growth season temperatures was calculated in relation to the mean $\delta^{13}C$ value for the entire core (−26.25‰), using the factor of −0.97 ± 0.23‰/°C as calibrated by Skrzypek et al. (2011). Seven major periods can be distinguished (Fig. 11):

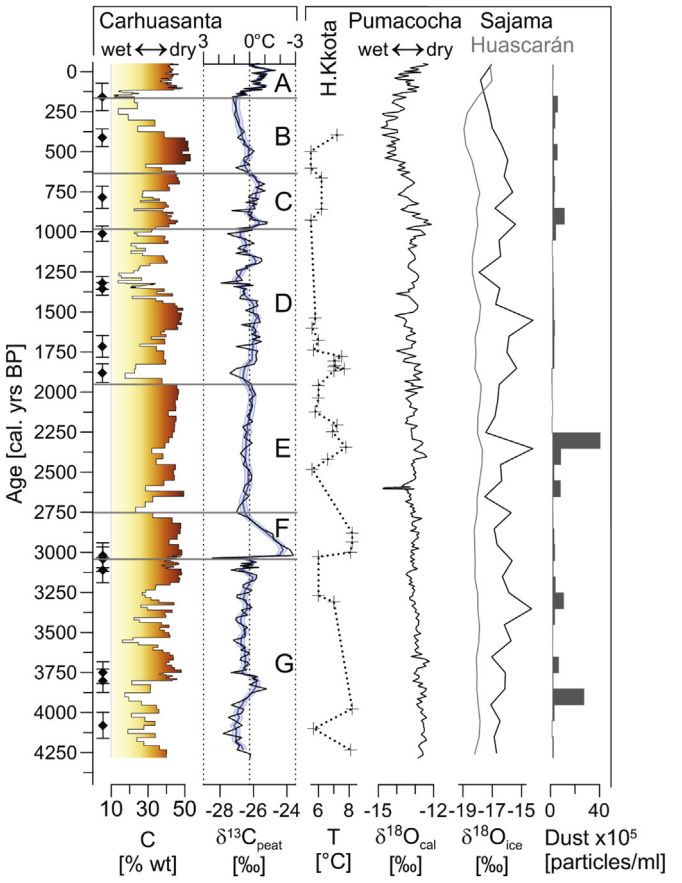

Fig. 11. The comparison of selected proxies in the core with other records in the Central Andes. The most prominent change in $\delta^{13}C$ value reflects a global climate event around 2.8 cal. ka BP. The temperature of growth season was about 2 °C lower than today during this short-term episode in the study area. The time intervals A to G are described in the text. Diamonds and error bars show the age and uncertainty of our data. Paleotemperatures for Hichu Kkota after Roux et al. (1987), $\delta^{18}O$ records and total dust concentrations based on NOAA datasets (Sowers and Campen, 2001; Thompson, 2001; Bird et al., 2011a,b). The Pumacocha $\delta^{18}O$ record (Bird et al., 2011a) is smoothed with a 7-point running average.

G) 4280–3040 cal. yrs BP (BC 2330–1090) – a moderately warm and relatively moist period with variable temperatures ranging from −1.0 below to +1.6 °C above the long term mean. The mean temperature in this period is ~0.3 °C higher than the mean temperature for the whole 4.3 ka, which is consistent with a proxy record from Hichu Kkota in the Eastern Cordillera where Roux et al. (1987) reveal a similar (0.4 °C) temperature difference between the period 4.3–3.0 ka and the Late Holocene. The most prominent climate change during this period occurred between 4130 and 3850 cal. yrs BP (BC 2180–1900) when the temperature decreased by more than 1.5 °C. This episode coincides with an abrupt increase in dust content in the Sajama ice core (Thompson et al., 1998; Sowers and Campen, 2001) and with a drop of benthic diatoms in the Lake Titicaca (Tapia et al., 2003). These changes were tentatively linked with the more pronounced ENSO regime (Sun, 2000), an austral summer insolation minimum and the subsequent weakening of the SASM (Tapia et al., 2003). The relatively moist conditions in the Carhuasanta valley between 4.2 and 3.2 ka are consistent with an inferred humid period on the Pacific slope of the Andes (Baied and Wheeler, 1993; Holmgren et al., 2001; Placzek et al., 2001) contradicting drier climate at higher elevations of the Western Cordillera (Thompson et al., 1998; Kuentz et al., 2012). A temporary increase in aridity in the Carhuasanta valley after 3820 cal. yrs BP (BC 1870) follows an abrupt dust event in the Sajama ice core and matches the most prominent $\delta^{18}O$ fluctuation in the Pumacocha record before 2.6 ka (Fig. 11). A shift to drier conditions after 3260 cal. yrs BP (BC 1310) is consistent with enhanced dust concentration and increased $\delta^{18}O$ values in the Sajama record. Around this time, a return to the more humid climate after the Middle Holocene arid phase occurred on the Altiplano and in the Eastern Cordillera (Abbott et al., 2003; Williams et al., 2011a).

F) 3040–2750 cal. yrs BP (BC 1090–800) – this period starts with a rapid warming by ~2.8 °C (−28.45‰ minimum value for the core) followed by an abrupt cooling by ~4.8 °C (−23.62‰ maximum $\delta^{13}C$ in the core) to the temperatures at least 2 °C lower than the mean for the Late Holocene; it then again increases progressively by ~3.2 °C to the values close to the mean of the G period. The high temperatures at the beginning of this period are reflected in enhanced accumulation rate of organic matter, which belongs to the highest within the core. However, for most of the time this is the coldest period recorded in the core. Only the core section at 522.5–500 cm (3020–2780 cal. yrs BP, BC 1070–830) shows a correlation between $\delta^{13}C$–$\delta^{15}N$; this correlation is highly significant and strong ($R^2 = 0.94$, $p < 0.001$). These findings may suggest that the preservation of organic matter of the peat is low during this period, which may also indicate dry condition and a dropping water level permitting advanced decomposition. Dry conditions are also confirmed by low C%, except for the last three decades when moisture increased. These exceptionally strong and rapid climatic changes around 2800 cal. yrs BP match an increase in pollen concentrations in the Coropuna peat core, related to increased precipitation (Kuentz et al., 2012). The inferred temperature changes are consistent with the most abrupt temperature excursion in the Hichu Kkota record (Roux et al., 1987) and the timing of the changes coincides with the Quelccaya ice cap record (Thompson et al., 2000), lake level oscillations in the Eastern Cordillera (Chepstow-Lusty et al., 2003; Hillyer et al., 2009) and with the start of Andean Pollen Zone VII in the Central and Northern Andes (Stahl, 2006). Moreover, these climate changes match the timing of the climate event around 2.8 cal. ka BP that was described initially in European peat bogs (Van Geel et al., 1996) and attributed to the changes in solar activity and oceanic circulation (Renssen et al., 2006). Recent reports provided evidence for a major climate shift in both the northern and southern hemispheres, implying global nature of the event (Chambers et al., 2007; Kroonenberg et al., 2007; Van der Putten et al., 2012 and reference therein). Most of the reported evidence is based on well-dated peat records in high-latitudes, whereas only indirect proxies were available from low-latitudes. In the sub/tropical South America, the 2.8 event was linked with a sudden temperature decline and a subsequent treeline shifts in the Colombian Andes, northern Chile and the Brazilian Highlands (van Geel and Renssen, 1998). The most prominent change in the *Distichia* peat core from the Carhuasanta valley represents the first evidence for the 2.8 event in the Western Cordillera of the Central Andes constrained by AMS ^{14}C data.

E) 2750–1950 cal. yrs BP (BC 800–0) – a mostly dry period with relatively stable temperatures close to the mean for the core, varying within −0.4–0.6 °C around the mean temperature for the core. A small difference (0.2 °C) in the mean temperatures for this period and the Late Holocene is also recorded in the Hichu Kkota peat core, which suggests, by contrast, much more variable temperatures in the Eastern Cordillera (Fig. 11). Inferred drier conditions in the study area are consistent with increased dust levels in the Sajama ice core during the first half of this

period (Thompson et al., 1998). The aridity temporarily decreased around 2610 cal. yrs BP (BC 660) when $\delta^{18}O$ values dropped in the Pumacocha record (Fig. 11). The beginning of an extended dry period (2350–1950 cal. yrs BP, BC 400–0) in the Carhuasanta valley is consistent with increased $\delta^{18}O$ values and the highest concentration of dust in the Sajama ice core (Ramirez et al., 2003). By contrast, a shift to wetter conditions occurred in the Eastern Cordillera around 2.3–2.2 ka BP (Abbott et al., 2003; Bird et al., 2011b).

D) 1950–980 cal. yrs BP (AD 0–970) – a mostly warm period with highly variable temperatures ranging from about −0.8 up to 1.7 °C above the mean for the core. An initial warm (+0.5 °C) and wetter episode around 1880 cal. yrs BP (AD 70) was followed by relatively dry conditions and stable temperatures close to the mean for the core until ~1450 cal. yrs BP (AD 500). Subsequently, two prominent warm and wetter excursions occurred, culminating around 1320 and 1010 cal. yrs BP (AD 630 and 940). The earlier of these episodes belongs to the warmest and wettest periods, which is also indicated by the most rapid accumulation of peat (8.1 mm yr^{-1}) within the core. Several horizons have high inorganic content, suggesting variable hydrological regimes. The correlation between $\delta^{13}C$ and C% is highly significant ($p < 0.001$) and strong ($R^2 = 0.55$), suggesting frequent waterlogging of the bog and the highest deposition of inorganic material during the warmest periods. The overall trend towards warmer conditions in the Carhuasanta valley in this period is consistent with observed temperature increase between ~2.2 and 0.9 cal. ka BP around Coropuna (Kuentz et al., 2012). The warm episode at the beginning of this period matches the timing of an abrupt temperature increase of 1.7 °C in the Hichu Kkota record in the Eastern Cordillera (Fig. 11) and the subsequent fluctuating temperatures coincide with the onset of highly variable ENSO activity (Fig. 2). The changes in humidity are in general agreement with the Sajama $\delta^{18}O$ record (Fig. 11) and the last dry episode around 1070 cal. yrs BP (AD 880) is also recorded in the Quelccaya and Pumacocha $\delta^{18}O$ records, which imply considerably weakened SASM and dry conditions in the Eastern Cordillera until AD 1100 (Bird et al., 2011a).

C) 980–640 cal. yrs BP (AD 970–1310) – a relatively cold period, with temperatures mostly below the average for the core, with variation between −1.1 and 1.1 °C. A few wet episodes within the predominantly dry period are associated with warmer phases occurring around 870 cal. yrs BP (AD 1085) and 780 cal. yrs BP (AD 1170). The $\delta^{13}C$ record confirms predominantly cold conditions in the Central Andes in this period which was by 0.7 °C colder than the Late Holocene mean value according to the paleotemperature record from Hichu Kkota. The initial cooling between 980 and 940 cal. yrs BP (AD 970–1010) in the Carhuasanta valley corresponds with colder conditions observed around Coropuna (Kuentz et al., 2012) and Hichu Kkota (Fig. 11). The timing of the warmer phases matches the "Medieval Warm Period" identified in proglacial lakes in the Western Cordillera (Stansell et al., 2013) and ammonium (NH_4^+) record from Nevado Illimani in the Eastern Bolivian Andes (Kellerhals et al., 2010). The predominantly dry conditions during this period are in good agreement with increased $\delta^{18}O$ in the Huascarán and Sajama ice cores (Thompson et al., 1995, 1998), Pumacocha lake sediments (Bird et al., 2011a) and Huagapo Cave (Kanner et al., 2013). Moreover, a variety of archives within the South American monsoon belt indicate a weaker SASM in this period (Vuille et al., 2012). The above-mentioned wet episodes are consistent with reduced dust concentrations in the ice cores that were attributed to more humid conditions during this period (Thompson et al., 2006). The dry conditions after 740 cal. yrs BP (AD 1210) coincide with the extended dry period 700–640 cal. yrs BP (AD 1250–1310) described in the Quelccaya ice core (Thompson et al., 1985).

B) 640–155 cal. yrs BP (AD 1310–1795) – a period of progressive warming, with the highest temperatures at the end ~1.0 °C above the core mean. The climate was dry until 430 cal. yrs BP (AD 1520), when it changed progressively to a wet phase. The warming trend observed in this period in the Carhuasanta peat contradicts the assumption of predominantly cold conditions during the LIA interval inferred from glacier advances in the 14th to 17th centuries (e.g. Jomelli et al., 2009). However, the relation between the temperature and glacier fluctuations in the Western Cordillera remains unclear. Instead of temperature, the precipitation has been mentioned repeatedly as the main climate control of glacier mass balance in the Central Andes (e.g. Rabatel et al., 2008). The diatom assemblages in the Hichu Kkota show cold conditions until ~500 cal. yrs BP followed by a temperature increase, which does agree with the general trend in the Carhuasanta peat (Fig. 11). In contrast to our record, NH_4^+ concentrations in the Illimani ice core suggest colder conditions from the 15th to 18th century in the Eastern Cordillera (Kellerhals et al., 2010). The wet conditions observed in the study area between 370 and 115 cal. yrs BP (AD 1580–1835) are consistent with pollen records and tree-rings reconstructions in the Western Cordillera (Liu et al., 2005; Morales et al., 2012) but started later than the wet period in the Eastern Cordillera according to the Pumacocha (AD 1400–1820; Bird et al., 2011a) and Quelccaya $\delta^{18}O$ records (AD 1520–1680; Thompson et al., 2013).

A) 155–0 cal. yrs BP (after 1795) – the second coldest period observed over the last 4280 years is wet until 115 cal. yrs BP (AD 1835) and then becomes drier. The temperature decreases by ~2 °C between 155 and 85 cal. yrs BP (AD 1795–1865) and then fluctuates until 1960 when it starts increasing rapidly. The temperature drop in the 19th century has not been previously reported in the Western Cordillera. The NH_4^+ record from Illimani that represents the only regional proxy for temperature reconstruction reveals a predominant warming in the Eastern Cordillera during this period (Kellerhals et al., 2010). A significant increase in the temperature in the last five decades is documented by the historical temperature records that indicate a gradual warming since 1939 (Vuille et al., 2008). The rapid warming may account for increased accumulation of organic matter, which has the mean rate of 7.5 mm yr^{-1} for this period. The high value of accumulation rate may be also influenced by lower compression of slightly decomposed peat below the peat bog surface compared to the lower parts of the core. However, similarly high values calculated for the warm episodes around 3110–3030 cal. yrs BP and 1350–1320 cal. yrs BP (BC 1160–1080 and AD 600–630) suggest that primary production and/or deposition of peat are controlled by temperature conditions. Evidence of climatic control on *Distichia* peat accumulation has been recently reported from the Northern Andes (Benavides et al., 2013). The shift from wet to drier conditions in the Carhuasanta valley around 115 cal. yrs BP (AD 1835) contradicts the results of the regional paleoclimate reconstruction that suggests a long-term drought to AD 1818 and subsequent increase in precipitation (Morales et al., 2012). By contrast, the drier conditions after AD 1835 are consistent with reduced precipitation indicated in the high-resolution pollen record from Sajama (Liu et al., 2005). In the Eastern Cordillera, an increase in aridity started after 130 cal. yrs BP (AD 1820) and the most arid conditions occurred after 50 cal. yrs BP (AD 1900; Bird et al., 2011a).

6. Conclusions

The peat core from the Carhuasanta valley in the Western Cordillera of southern Peru provides evidence for climate variability over the Late Holocene. Relatively warm and moist climate prevailed from 4280 to 3040 cal. yrs BP (BC 2330–1090) when only a minor shift to colder and drier conditions between 4130 and 3850 cal. yrs BP (BC 2180–1900) occurred. A prominent fluctuation of $\delta^{13}C$ values between 3040 and 2750 cal. yrs BP (BC 1090–800) indicates the most significant climate event in the Late Holocene. The event started with climate warming by ~2.8 °C which was followed by a rapid cooling by ~4.8 °C to the temperatures at least 2 °C lower than the mean for the Late Holocene. At the end of the event the temperature increased by ~3.2 °C and predominantly dry conditions turned to a short wet phase. Relatively stable climatic conditions prevailed after this event until around 1950 cal. yrs BP when the climate turned to a highly variable mode. Prominent warm and wetter episodes occurred around 1880, 1320 and 1010 cal. yrs BP (AD 70, 630 and 940). After 1010 cal. yrs BP temperature and humidity decreased rapidly and predominantly colder and relatively drier conditions prevailed until 640 cal. yrs BP (AD 1310). Sustained warming and increase in humidity started after 640 cal. yrs BP and prevailed until 115 cal. yrs BP (AD 1835). Predominantly colder and drier conditions followed in the 19th century and in the first half of the 20th century.

The established $\delta^{13}C$ peat record represents the first continuous proxy for temperature in the Western Cordillera dated by the AMS ^{14}C. The record is consistent with environmental proxies from nearby Coropuna (Kuentz et al., 2012) and with the diatom-based paleotemperature record from Hichu Kkota peat in the Eastern Cordillera (Roux et al., 1987). The timing for the most prominent temperature fluctuation observed in the Carhuasanta peat core correlates with the climate event around 2.8 cal. ka BP which is recorded in many peat-based records in the northern hemisphere, South Africa, South America and sub-Antarctic islands (e.g. Lewis, 2005; Chambers et al., 2007; Kroonenberg et al., 2007; Van der Putten et al., 2012). The minor cooling episode between 4.1 and 3.9 cal. ka BP coincides with the dust record in the Sajama ice core (Sowers and Campen, 2001) and the diatoms changes in Lake Titicaca (Tapia et al., 2003). The cold episode after 1 cal. ka BP is consistent with the pollen record from Coropuna (Kuentz et al., 2012) and the trend towards warmer conditions since the middle of the 20th century matches the historical temperature records (e.g. Vuille et al., 2008).

The relatively wet conditions inferred for the study area until 3.2 cal. ka BP match a humid period on the Pacific slope of the Andes (Holmgren et al., 2001; Placzek et al., 2001) but contradict arid phase at higher elevations of the Western Cordillera, Altiplano and Eastern Cordillera (Abbott et al., 2003; Williams et al., 2011a; Kuentz et al., 2012). A temporary increase in aridity after 3.8 cal. ka BP is consistent with fluctuations in the Sajama dust record and the Pumacocha $\delta^{18}O$ signature (Thompson et al., 1998; Bird et al., 2011b). Extended drier periods in the Carhuasanta valley around 3.2–2.8 and 2.3–2.0 cal. ka BP follow increased $\delta^{18}O$ values and dust levels in the Sajama ice core (Sowers and Campen, 2001; Ramirez et al., 2003) and shifts to wetter conditions in the Eastern Cordillera (Williams et al., 2011a; Bird et al., 2011b). The observed changes in humidity after 1.8 cal. ka BP are in general agreement with the Huascarán and Sajama $\delta^{18}O$ records (Thompson et al., 1995, 1998), pollen and tree-rings reconstructions in the Western Cordillera (Liu et al., 2005; Morales et al., 2012). Abrupt increases in aridity around 1.0 and 0.1 cal. ka BP interleaved with a prominent wet episode between 0.4 and 0.1 cal. ka BP also match reconstructed SASM precipitation in the Eastern Cordillera (Bird et al., 2011a; Vuille et al., 2012; Kanner et al., 2013).The described reconstructions of the past climate variations show that *Distichia* peat represents a unique archive of environmental changes. The relative change in $\delta^{13}C$ value of well-preserved *Distichia* macrofossils in peat reflects the relative changes in the air temperature of the growth season and $\delta^{13}C$ relation with C% of organic matter is indicative of moisture conditions. More positive $\delta^{13}C$ values and higher C% are linked with lower temperatures and drier conditions at the study site and vice versa. The climate conditions have an impact on accumulation rate and decomposition of *Distichia* peat. The mean values of the accumulation rate within the core range from 0.7 to 3.9 mm yr^{-1} for most of the last ~4.3 ka except for the periods with increased temperature and/or moisture conditions. The warmest and mostly wetter periods are reflected by the significantly higher mean accumulation rate of 7.3–8.1 mm yr^{-1} implying a positive effect of temperature and water table level on primary peat production and decomposition. The observed relation between climate conditions and accumulation of organic matter is consistent with the recent conclusions about the impact of climate on *Sphagnum* (Chivers et al., 2009; Loisel et al., 2012; and references therein) and *Distichia* peat (Benavides et al., 2013).

Based on the relationships between climate conditions and accumulation of *Distichia* peat, the $\delta^{13}C$ values recorded in the peat cores can be used as a high-resolution proxy for paleoclimate reconstructions. *Distichia* peat accumulated during the Holocene in the high Andean environment is allowing paleoclimate reconstructions even in regions where alternative sedimentary records are scarce. Therefore, the wetlands developed along the Andean range from the low- to mid-latitudes may represent the best available widespread perspective archives in the South America to investigate past climate changes.

Acknowledgements

Funding for this work was provided by the Czech Science Foundation (project no. 205/07/831). Grzegorz Skrzypek is supported by a Future Fellowship from the Australian Research Council (FT110100352). We thank Anibal Lajo (Universidad Nacional de San Augustin, Arequipa, Peru) for logistic support.

References

Abbott, M.B., Wolfe, B.B., Wolfe, A.P., Seltzer, G.O., Aravena, R., Mark, B.G., Polissar, P.J., Rodbell, D.T., Rowe, H.D., Vuille, M., 2003. Holocene paleohydrology and glacial history of the central Andes using multiproxy lake sediment studies. Palaeogeogr. Palaeoclimatol. Palaeoecol. 194 (1–3), 123–138.

Alcalá, J., Palacios, D., Zamorano, J.J., 2010. Glacial Recession in the Tropical Andes from the Little Ice Age: the Case of Ampato Volcanic Complex (Southern Peru), 6th Alexander von Humboldt International Conference, AvH6–H10.

Andrus, C.F.T., Crowe, D.E., Sandweiss, D.H., Reitz, E.J., Romanek, C.S., 2002. Otolith $\delta^{18}O$ record of mid-Holocene sea surface temperatures in Peru. Science 295, 1508–1511.

Argollo, J., Mourguiart, P., 2000. Late Quaternary climate history of the Bolivian Altiplano. Quatern. Int. 72, 37–51.

Baied, C.A., Wheeler, J.C., 1993. Evolution of high Andean Puna ecosystems: environment, climate, and culture change over the last 12,000 years in the Central Andes. Mt. Res. Dev. 13 (2), 145–156.

Baker, P.A., Seltzer, G.O., Fritz, S.C., Dunbar, R.B., Grove, M.J., Tapia, P.M., Cross, S.L., Rowe, H.D., Broda, J.P., 2001. The history of South American tropical precipitation for the past 25,000 years. Science 291, 640–643.

Balslev, H., 1996. Juncaceae. New York Botanical Garden Press, Bronx.

Benavides, J.C., Vitt, D.H., Wieder, K.H., 2013. The influence of climate change on recent peat accumulation patterns of *Distichia muscoides* cushion bogs in the high-elevation tropical Andes of Colombia. J. Geophys. Res. Biogeo. 118, 1627–1635.

Bershaw, J., Garzione, C.N., Higgins, P., MacFadden, B.J., Anaya, F., Alvarenga, H., 2010. Spatial-temporal changes in Andean plateau climate and elevation from stable isotopes of mammal teeth. Earth Planet. Sci. Lett. 289, 530–538.

Bird, B.W., Abbott, M.B., Vuille, M., Rodbell, D.T., Stansell, N.D., Rosenmeier, M.F., 2011a. A 2300-year-long annually resolved record of the South American summer monsoon from the Peruvian Andes. Proc. Natl. Acad. Sci. U. S. A. 108, 8583–8588.

Bird, B.W., Abbott, M.B., Rodbell, D.T., Vuille, M., 2011b. Holocene tropical South American hydroclimate revealed from a decadally resolved lake sediment $\delta^{18}O$ record. Earth Planet. Sci. Lett. 310, 192–202.
Brader, A.V., van Winden, J.F., Bohncke, S.J.P., Beets, C.J., Reichart, G.J., de Leeuw, J.W., 2010. Fractionation of hydrogen, oxygen and carbon isotopes in *n*-alkanes and cellulose of three *Sphagnum* species. Org. Geochem. 41, 1277–1284.
Bromley, G.R.M., Hall, B.L., Schaefer, J.M., Winckler, G., Todd, C.E., Rademaker, K.M., 2011. Glacier fluctuations in the southern Peruvian Andes during the late-glacial period, constrained with cosmogenic ^{3}He. J. Quat. Sci. 26, 37–43.
Bronk Ramsey, C., 2009. Bayesian analysis of radiocarbon dates. Radiocarbon 51 (1), 337–360.
Buffen, A.M., Thompson, L.G., Mosley-Thompson, E., Huh, K.-I., 2009. Recently exposed vegetation reveals Holocene changes in the extent of the Quelccaya ice cap, Peru. Quat. Res. 72, 157–163.
Bush, M.B., Silman, M.R., Urrego, D.H., 2004. 48,000 years of climate and forest change in a biodiversity hotspot. Science 303, 827–829.
Bush, M.B., Hansen, B.C.S., Rodbell, D.T., Seltzer, G.O., Young, K.R., León, B., Abbott, M.B., Silman, M.R., Gosling, W.D., 2005. A 17 000-year history of Andean climate and vegetation change from Laguna de Chochos, Peru. J. Quat. Sci. 20, 703–714.
Candiotti de Los Rios, H., Noble, D.C., McKee, E.H., 1990. Geologic setting and epithermal silver veins of the Arcata district, Southern Peru. Econ. Geol. 85, 1473–1490.
Carré, M., Azzoug, M., Bentaleb, I., Chase, B.M., Fontugne, M., Jackson, D., Ledru, M.-P., Maldonado, A., Sachs, J.P., Schauer, A.J., 2012. Mid-Holocene mean climate in the south eastern Pacific and its influence on South America. Quatern. Int. 253, 55–66.
Chambers, F.M., Mauquoy, D., Brain, S.A., Blaauw, M., Daniell, J.R.G., 2007. Globally synchronous climate change 2800 years ago: proxy data from peat in South America. Earth Planet. Sci. Lett. 253, 439–444.
Chapman, E.N., Kelly, T., 2013. Fortuna Silver Mines Inc.: Caylloma Property, Caylloma District, Peru. Fortuna Silver Mines Inc., Vancouver.
Chepstow-Lusty, A., Frogley, M.R., Bauer, B.S., Bush, M.B., Herrera, A.T., 2003. A late Holocene record of arid events from the Cuzco region, Peru. J. Quat. Sci. 18, 491–502.
Chivers, M.C., Turetsky, M.R., Waddington, J.M., Harden, J.W., McGuire, A.D., 2009. Effects of experimental water table and temperature manipulations on ecosystem CO_2 fluxes in an Alaskan boreal peatland. Ecosystems 12, 1329–1342.
Clapperton, C.M., 1983. The glaciation of the Andes. Quat. Sci. Rev. 2, 83–155.
Clement, A.C., Seager, R., Cane, M.A., 2000. Suppression of El Niño during the mid-Holocene by changes in the Earth's orbit. Paleoceanography 15, 731–737.
Cross, S.L., Baker, P.A., Seltzer, G.O., Fritz, S.C., Dunbar, R.B., 2000. A new estimate of the Holocene lowstand level of Lake Titicaca, central Andes, and implications for tropical paleohydrology. Holocene 10, 21–32.
Davila, D., 1988. Geología del Cuadrángulo de Caylloma. Instituto Geológico Minero y Metalúrgico, Lima.
Dornbusch, U., 2002. Pleistocene and present day snowlines rise in the Cordillera Ampato, Western Cordillera, southern Peru (15°15′–15°45′ S and 77°30′–77°15′ W). Neues Jahrb. Geol. P. A. 225, 103–126.
Echavarria, E., Nelson, E., Humphrey, J., Chavez, J., Escobedo, L., Iriondo, A., 2006. Geologic evolution of the Caylloma epithermal Vein District, Southern Perú. Econ. Geol. 101, 843–863.
Engel, Z., 2002. Geomorphology of the Amazon source area in the Cordillera Chila. Acta Mont. Ser. A 19 (123), 91–108.
Engel, Z., Skrzypek, G., Paul, D., Drzewicki, W., Nývlt, D., 2010. Sediment lithology and stable isotope composition of organic matter in a core from a cirque in the Krkonoše Mountains, Czech Republic. J. Paleolimnol. 43 (4), 609–624.
Falvey, M., Garreaud, R., 2005. Moisture variability over the South American Altiplano during the South American Low Level Jet Experiment (SALLJEX) observing season. J. Geophys. Res. 110, D22105.
Fontugne, M., Usselmann, P., Lavallée, D., Julien, M., Hatté, C., 1999. El Niño variability in the coastal desert of southern Peru during the mid-Holocene. Quat. Res. 52 (2), 171–179.
Fritz, S.C., Baker, P.A., Ekdahl, E., Seltzer, G.O., Stevens, L.R., 2010. Millennial-scale climate variability during the Last Glacial period in the tropical Andes. Quat. Sci. Rev. 29, 1017–1024.
Garreaud, R.D., 2009. The Andes climate and weather. Adv. Geosci. 7, 3–11.
Garreaud, R.D., Vuille, M., Clement, A.C., 2003. The climate of the Altiplano: observed current conditions and mechanisms of past changes. Palaeogeogr. Palaeoclimatol. Palaeoecol. 194, 5–22.
Garreaud, R.D., Vuille, M., Compagnucci, R., Marengo, J., 2009. Present-day South American climate. Palaeogeogr. Palaeoclimatol. Palaeoecol. 281, 180–195.
Gonzalez, S., Jones, J.M., Williams, D.L., 1999. Characterization of tephras using magnetic properties: an example from SE Iceland. In: Firth, C.R., McGuire, J. (Eds.), Volcanoes in the Quaternary. Geological Society, London, pp. 125–145.
Gosling, W.D., Bush, M.B., Hanselman, J.A., Chepstow-Lusty, A., 2008. Glacial-interglacial changes in moisture balance and the impact on vegetation in the southern hemisphere tropical Andes (Bolivia/Peru). Palaeogeogr. Palaeoclimatol. Palaeoecol. 259, 35–50.
Graf, K., 1992. Pollendiagramme aus den Anden: eine Synthese zur Klimageschichte und Vegetationsentwicklung seit der letzten Eiszeit. Geographisches Institut der Universität Zürich, Zürich.
Graf, K., 1994. Discussion of palynological methods and paleoclimatical interpretations in northern Chile and the whole Andes. Rev. Chil. Hist. Nat. 67, 405–415.
Graf, K., 1999. Zur Datierung letzteiszeitlicher Moränen und Seesedimente in den tropischen Anden. Bamb. Geogr. Schr. 19, 63–75.
Grosjean, M., Santoro, C.M., Thompson, L.G., Núñez, L., Standen, V.G., 2007. Mid-Holocene climate and culture change in the South Central Andes. In: Anderson, D.G., Maasch, K.A., Sandweiss, D.H. (Eds.), Climate Change and Cultural Dynamics: a Global Perspective on Mid-Holocene Transitions. Elsevier, Amsterdam, pp. 51–115.
Hansen, B.C.S., Rodbell, D.T., 1995. A Late-glacial/Holocene pollen record from the eastern Andes of Northern Peru. Quat. Res. 44, 216–227.
Hansen, B.C.S., Wright, H.E., Bradbury, J.P., 1984. Pollen studies in the Junín area, central Peruvian Andes. Geol. Soc. Am. Bull. 95, 1454–1465.
Hansen, B.C.S., Seltzer, G.O., Wright, H.E., 1994. Late Quaternary vegetational change in the central Peruvian Andes. Palaeogeogr. Palaeoclimatol. Palaeoecol. 109 (2), 263–285.
Hastenrath, S.L., 1967. Observations on the snow line in the Peruvian Andes. J. Glaciol. 6, 541–550.
Hillyer, R., Valencia, B.G., Bush, M.B., Silman, M.R., Steinitz-Kannan, M., 2009. A 24,700-year paleolimnological history from the Peruvian Andes. Quat. Res. 71, 71–82.
Hoffmann, G., Ramirez, E., Taupin, J.D., Francou, B., Ribstein, P., Delmas, R., Dürr, H., Gallaire, R., Simões, J., Schotterer, U., et al., 2003. Coherent isotope history of Andean ice cores over the last century. Geophys. Res. Lett. 30, 1179.
Hogg, A.G., Hua, Q., Blackwell, P.G., Niu, M., Buck, C.E., Guilderson, T.P., Heaton, T.J., Palmer, J.G., Reimer, P.J., Reimer, R.W., Turney, C.S.M., Zimmerman, S.R.H., 2013. SHCal13 Southern Hemisphere calibration, 0–50,000 years cal BP. Radiocarbon 55 (4), 1889–1903.
Holmgren, C.A., Betancourt, J.L., Rylander, K.A., Roque, J., Tovar, O., Zeballos, H., Linares, E., Quade, J., 2001. Holocene vegetation history from fossil rodent middens near Arequipa, Peru. Quat. Res. 56 (2), 242–251.
Janský, B., Engel, Z., Kocum, J., Šefrna, L., Česák, J., 2011. The Amazon River headstream area in the Cordillera Chila, Peru: hydrographic, hydrological and glaciological conditions. Hydrol. Sci. J. 56 (1), 138–151.
Jomelli, V., Favier, V., Rabatel, A., Brunstein, D., Hoffmann, G., Francou, B., 2009. Fluctuations of glaciers in the tropical Andes over the last millennium and palaeoclimatic implications: a review. Palaeogeogr. Palaeoclimatol. Palaeoecol. 281 (3), 269–282.
Juvigné, E., Thouret, J.-C., Gilot, E., Gourgaud, A., Legros, F., Uribe, M., Graf, K., 1997. Etude téphrostratigraphique et bioclimatique du Tardiglaciaire et de l'Holocène de la Laguna Salinas, Pérou méridional. Géogr. Phys. Quat. 51 (2), 219–231.
Juvigné, E., Thouret, J.-C., Loutsch, I., Lamadon, S., Frechen, M., Fontugne, M., Rivera, M., Davila, J., Mariño, J., 2008. Retombées volcaniques dans des tourbières et lacs autour du massif des Nevados Ampato et Sabancaya (Pérou Méridional, Andes Centrales). Quaternaire 19 (2), 157–173.
Kanner, L.C., Burns, S.J., Cheng, H., Edwards, R.L., 2012. High-latitude forcing of the South American summer monsoon during the Last Glacial. Science 335, 570–573.
Kanner, L.C., Burns, S.J., Cheng, H., Edwards, R.L., Vuille, M., 2013. High-resolution variability of the South American summer monsoon over the last seven millennia: insights from a speleothem record from the central Peruvian Andes. Quat. Sci. Rev. 75 (1), 1–10.
Kaser, G., 2001. Glacier–climate interaction at low-latitudes. J. Glaciol. 47, 195–204.
Kellerhals, T., Brütsch, S., Sigl, M., Knüsel, S., Gäggeler, H.W., Schwikowski, M., 2010. Ammonium concentration in ice cores: a new proxy for regional temperature reconstruction. J. Geophys. Res. 115 (D16), D16123.
Koutavas, A., Lynch-Stieglitz, J., 2004. Variability of the marine ITCZ over the Eastern Pacific during the past 30,000 years regional perspective and global context. In: Diaz, H.F., Bradley, R.S. (Eds.), The Hadley Circulation: Present, Past, and Future. Kluwer Academic Press, Dordrecht.
Kroonenberg, S.B., Abdurakhmanov, G.M., Badyukova, E.N., van der Borg, K., Kalashnikov, A., Kasimov, N.S., Rychagov, G.I., Svitoch, A.A., Vonhof, H.B., Wesselingh, F.P., 2007. Solar-forced 2600 BP and Little Ice Age highstands of the Caspian Sea. Quat. Int. 173-174, 137–143.
Kuentz, A., Ledru, M.-P., Thouret, J.C., 2012. Environmental changes in the highland of the western Andean Cordillera (south Peru) during the Holocene. Holocene 22, 1215–1226.
Kull, C., Grosjean, M., 2000. Late Pleistocene climate conditions in the north Chilean Andes drawn from a climate glacier model. J. Glaciol. 46, 622–632.
Lagos, P., Silva, Y., Nickl, E., Mosquera, K., 2008. El Niño – related precipitation variability in Perú. Adv. Geosci. 14, 231–237.
Lajo, A., Nuñez Juarez, S.A., 2008. Estructura y evolución geológicas. In: Janský, B., et al. (Eds.), Los Orígenes del Amazonas. Ottovo Nakladatelství, Praha, pp. 159–166.
Latorre, C., Betancourt, J.L., Rylander, K.A., Quade, J., 2002. Vegetation invasions into absolute desert: a 45,000-year rodent midden record from the Calama–Salar de Atacama basins, northern Chile (22–24°S). Geol. Soc. Am. Bull. 114, 349–366.
Lavado Casimiro, W.S., Labat, D., Ronchail, J., Espinoza, J.C., Guyot, J.L., 2013. Trends in rainfall and temperature in the Peruvian Amazon–Andes basin over the last 40 years (1965–2007). Hydrol. Process. 27, 2944–2957.
Ledru, M.P., Jomelli, V., Bremond, L., Ortuño, T., Cruz, P., Bentaleb, I., Sylvestre, F., Kuentz, A., Beck, S., Martin, C., Paillès, C., Subitani, S., 2013. Evidence of moist niches in the Bolivian Andes during the mid-Holocene arid period. Holocene 23 (11), 1547–1559.
Lenters, J.D., Cook, K.H., 1997. On the origin of the Bolivian high and related circulation features of the South American climate. J. Atmos. Sci. 54, 656–677.

Lewis, C.A., 2005. Late glacial and Holocene palaeoclimatology of the Drakensberg of the eastern Cape, South Africa. Quat. Int. 129 (1), 33–48.
Liu, K., Reese, C.A., Thompson, L.G., 2005. Ice-core pollen record of climatic changes in the central Andes during the last 400 years. Quat. Res. 64 (2), 272–278.
Liu, K., Reese, C.A., Thompson, L.G., 2007. A potential pollen proxy for ENSO derived from the Sajama ice core. Geophys. Res. Lett. 34, L09504.
Loader, N.J., McCarroll, D., van der Knaap, W.O., Robertson, I., Gagen, M., 2007. Characterizing carbon isotopic variability in *Sphagnum*. Holocene 17, 403–410.
Loisel, J., Gallego-Sala, A.V., Yu, Z., 2012. Global-scale pattern of peatland *Sphagnum* growth driven by photosynthetically active radiation and growing season length. Biogeosciences 9, 2737–2746.
Markgraf, V., 1989. Palaeoclimates in Central and South America since 18 000 BP based on pollen and lake-level records. Quat. Sci. Rev. 8, 1–24.
Martin, L., Bertaux, J., Corrège, T., Ledru, M.-P., Mourguiart, P., Sifeddine, A., Soubiès, F., Wirrmann, D., Suguio, K., Turcq, B., 1997. Astronomical forcing of contrasting rainfall changes in tropical South America between 12,400 and 8800 cal yr B.P. Quat. Res. 47, 117–122.
May, J.-H., Zech, R., Schellenberger, A., Kull, C., Veit, H., 2011. Quaternary environmental and climate changes in the Central Andes. In: Salfity, J.A., Marquillas, R.A. (Eds.), Cenozoic Geology of the Central Andes of Argentina. SCS Publisher, Salta, pp. 247–263.
Ménot-Combes, G., Combes, P.P., Burns, S.J., 2004. Climatic information from $\delta^{13}C$ in plants by combining statistical and mechanistic approaches. Holocene 14, 931–939.
Morales, M.S., Christie, D.A., Villalba, R., Argollo, J., Pacajes, J., Silva, J.S., Alvarez, C.A., Llancabure, J.C., Soliz Gamboa, C.C., 2012. Precipitation changes in the South American Altiplano since 1300 AD reconstructed by tree-rings. Clim. Past 8, 653–666.
Mosblech, N.A.S., Chepstow-Lusty, A., Valencia, B.G., Bush, M., 2012. Anthropogenic control of late-Holocene landscapes in the Cuzco region, Peru. Holocene 22, 1361–1372.
Moschen, R., Kühl, N., Rehberger, I., Lücke, A., 2009. Stable carbon and oxygen isotopes in sub-fossil *Sphagnum*: assessment of their applicability for palaeoclimatology. Chem. Geol. 259, 262–272.
Moy, C.M., Seltzer, G.O., Rodbell, D.T., Anderson, D.M., 2002. Variability of El Niño/Southern Oscillation activity at millennial timescales during the Holocene epoch. Nature 420, 162–165.
Munsell Soil Color Chart, 2000. GretagMacbeth, New Windsor.
Ostria, C., 1987. Végétation actuelle et fossile de haute altitude (exemple d'une vallée glaciaire: Hichu Kkota, Cordillère Royale des Andes de Bolivie). Geodynamique 2 (2), 109–111.
Paulo, A., Gałaś, A., 2008. Górnictwo i inne inwestycje w sąsiedztwie Kanionu Colca. Geologia 34 (2/1), 137–172.
Pella, E., 1990. Elemental organic analysis. Part 1. Historical developments. Am. Lab. 22 (3(Feb)), 116–125.
Perry, L.B., Seimon, A., Kelly, G.M., 2014. Precipitation delivery in the tropical high Andes of southern Peru: new findings and paleoclimatic implications. Int. J. Climatol. 34, 197–215.
Placzek, C., Quade, J., Betancourt, J.L., 2001. Holocene lake-level fluctuations of Lake Aricota, southern Peru. Quat. Res. 56, 181–190.
Placzek, C.J., Quade, J., Patchett, P.J., 2013. A 130 ka reconstruction of rainfall on the Bolivian Altiplano. Earth Planet. Sci. Lett. 363 (1), 97–108.
Rabatel, A., Francou, B., Jomelli, V., Naveau, P., Grancher, D., 2008. A chronology of the little ice age in the tropical Andes of Bolivia (16°S) and its implications for climate reconstruction. Quat. Res. 70, 198–212.
Ramirez, E., Hoffmann, G., Taupin, J.D., Francou, B., Ribstein, P., Caillon, N., Ferron, F.A., Landais, A., Petit, J.R., Pouyaud, B., Schotterer, U., Simões, J.C., Stievenard, M., 2003. A new Andean deep ice core from Nevado Illimani (6350 m), Bolivia. Earth Planet. Sci. Lett. 212, 337–350.
Reese, C., Liu, K., Thompson, L., 2013. An ice-core pollen record showing vegetation response to Late-glacial and Holocene climate changes at Nevado Sajama, Bolivia. Ann. Glaciol. 54 (63), 183–190.
Renssen, H., Goosse, H., Muscheler, R., 2006. Coupled climate model simulation of Holocene cooling events: oceanic feedback amplifies solar forcing. Clim. Past 2, 79–90.
Rodbell, D.T., 1992. Lichenometric and radiocarbon dating of Holocene glaciation, Cordillera Blanca Perú. Holocene 2, 19–29.
Rodbell, D.T., Seltzer, G.O., Anderson, D.M., Abbott, M.B., Enfield, D.B., Newman, J.H., 1999. An ~15000-year record of El Niño-driven alluviation in southwestern Ecuador. Science 283, 516–520.
Rodbell, D.T., Seltzer, G.O., Mark, B.G., Smith, J.A., Abbott, M.B., 2008. Clastic sediment flux to tropical Andean lakes: records of glaciation and soil erosion. Quat. Sci. Rev. 27, 1612–1626.
Rodbell, D.T., Smith, J.A., Mark, B.G., 2009. Glaciation in the Andes during the Lateglacial and Holocene. Quat. Sci. Rev. 28 (21), 2165–2212.
Roux, M., Servant-Vildary, S., Mello e Sousa, S.H., 1987. Diatomées et milieux aquatiques de Bolivie. application des methods statistiques à l'évolution des paléotempératures et des paléosalinités. Geodynamique 2 (2), 116–119.
Rowe, H.R., Guilderson, T.P., Dunbar, R.B., Sothon, J.R., Seltzer, G.O., Mucciarone, D.A., Fritz, S.C., Baker, P.A., 2003. Late Quaternary lake-level changes constrained by radiocarbon and stable isotope studies on sediment cores from Lake Titicaca, South America. Glob. Planet. Change 38, 273–290.
Schittek, K., Mächtle, B., Schäbitz, F., Forbriger, M., Wennrich, V., Reindel, M., Eitel, B., 2014. Holocene environmental changes in the highlands of the southern Peruvian Andes (14° S) and their impact on pre-Columbian cultures. Clim. Past Discuss. 10, 1707–1746.
Schwalb, A., Burns, S.J., Kelts, K., 1999. Holocene environments from stable isotope stratigraphy of ostracods and authigenic carbonate in Chilean Altiplano lakes. Palaeogeogr. Palaeoclimatol. Palaeoecol. 148, 153–168.
Seltzer, G., Rodbell, D., Burns, S., 2000. Isotopic evidence for late Quaternary climatic change in tropical South America. Geology 28, 35–38.
Seluchi, M., Garreaud, R., Norte, F., Saulo, A., 2006. Influence of the subtropical Andes on Baroclinic disturbances: a Cold Front case study. Mon. Weather Rev. 134 (11), 3317–3335.
Shotyk, W., Blaser, P., Grünig, A., Cheburkin, A.K., 2000. A new approach for quantifying cumulative, anthropogenic, atmospheric lead deposition using peat cores from bogs: Pb in eight Swiss peat bog profiles. Sci. Total Environ. 249 (1–3), 281–295.
Silva Dias, P.L., Turcq, B., Silva Dias, M.A.F., Braconnot, P., Jorgetti, T., 2009. Mid-Holocene climate of tropical South America: a model-data approach. In: Vimeux, F., Sylvestre, F., Khodri, M. (Eds.), Past Climate Variability in South America and Surrounding Regions. Springer, Heidelberg, pp. 259–282.
Skrzypek, G., 2013. Normalization procedures and reference material selection in stable HCNOS isotope analyses – an overview. Anal. Bioanal. Chem. 405, 2815–2823.
Skrzypek, G., Paul, D., 2006. $\delta^{13}C$ analyses of calcium carbonate: comparison between the GasBench and elemental analyzer techniques. Rapid Commun. Mass Spectrom. 20, 2915–2920.
Skrzypek, G., Kałużny, A., Wojtuń, B., Jędrysek, M.O., 2007. The carbon stable isotopic composition of mosses: a record of temperature variation. Org. Geochem. 38, 1770–1781.
Skrzypek, G., Sadler, R., Paul, D., 2010. Error propagation in normalization of stable isotope data: a Monte Carlo analysis. Rapid Commun. Mass Spectrom. 24, 2697–2705.
Skrzypek, G., Engel, Z., Chuman, T., Šefrna, L., 2011. *Distichia* peat – a new stable isotope paleoclimate proxy for the Andes. Earth Planet. Sci. Lett. 307, 298–308.
Skrzypek, G., Paul, D., Wojtuń, B., 2013. The altitudinal climatic effect on the stable isotope compositions of *Agave* and *Opuntia* in arid environments – a case study at the Big Bend National Park, Texas, USA. J. Arid Environ. 92, 102–112.
Smith, C.A., Lowell, T.V., Caffee, M.W., 2009. Late glacial and Holocene cosmogenic surface exposure age glacial chronology and geomorphological evidence for the presence of cold-based glaciers at Nevado Sajama, Bolivia. J. Quat. Sci. 24, 360–372.
Solomina, O., Jomelli, V., Kaser, G., Ames, A., Berger, B., Pouyaud, B., 2007. Lichenometry in the Cordillera Blanca, Peru: "Little Ice Age" moraine chronology. Glob. Planet. Change 59, 225–235.
Sowers, T.A., Campen, R.K., 2001. Sajama Ice Core Gas Composition Data. In: IGBP PAGES/World Data Center A for Paleoclimatology Data Contribution Series #2001-062. NOAA/NGDC Paleoclimatology Program, Boulder CO, USA.
Squeo, F.A., Warner, B.G., Aravena, R., Espinoza, D., 2006. Bofedales: high altitude peatlands of the Central Andes. Rev. Chil. Hist. Nat. 79 (2), 245–255.
Stahl, P.W., 2006. Archaeology in the Lowland American Tropics: Current Analytical Methods and Applications. Cambridge University Press, Cambridge.
Stansell, N.D., Rodbell, D.T., Abbott, M.B., Mark, B.G., 2013. Proglacial lake sediment records of Holocene climate change in the western Cordillera of Peru. Quat. Sci. Rev. 10, 1–14.
Strnad, L., Ettler, V., Mihaljevič, M., Hladil, J., Chrastný, V., 2009. Determination of trace elements in calcite using solution and laser ablation ICP-MS: calibration to SRM NIST glass and USGS MACS carbonate and application to real landfill calcites. Geostand. Geoanal. Res. 33, 347–355.
Sun, D., 2000. Global climate change and El Niño: a theoretical framework. In: Diaz, H.F., Markgraf, V. (Eds.), El Niño and the Southern Oscillation. Cambridge University Press, Cambridge, pp. 443–463.
Šefrna, L., 2008. Los suelos y la biósfera de la región de las nacientes del Amazonas. In: Janský, B., et al. (Eds.), Los Orígenes del Amazonas. Ottovo Nakladatelství, Praha, pp. 196–207.
Tapia, P.M., Fritz, S.C., Baker, P.A., Seltzer, G.O., Dunbar, R.B., 2003. A late quaternary diatom record of tropical climatic history from Lake Titicaca (Peru and Bolivia). Palaeogeogr. Palaeoclimatol. Palaeoecol. 194, 139–164.
ter Braak, C.J.F., Šmilauer, P., 2002. CANOCO Reference Manual and CanoDraw for Windows User's Guide: Software for Canonical Community Ordination (Version 4.5). Microcomputer Power, Ithaca, NY.
Thompson, L.G., 2001. Huascarán Ice Core Data. In: IGBP PAGES/World Data Center A for Paleoclimatology Data Contribution Series #2001-008. NOAA/NGDC Paleoclimatology Program, Boulder CO, USA.
Thompson, L.G., Mosley-Thompson, E., Bolzan, J.F., Koci, B.R., 1985. A 1500 year record of tropical precipitation recorded in ice cores from the Quelccaya Ice Cap, Peru. Science 229, 971–973.
Thompson, L.G., Mosley-Thompson, E., Davis, M.E., Lin, P.-N., Henderson, K.A., Cole-Dai, J., Bolzan, J.F., Liu, K., 1995. Late Glacial Stage and Holocene tropical ice core records from Huascarán, Peru. Science 269, 46–50.
Thompson, L.G., Davis, M.E., Mosley-Thompson, E., Sowers, T.A., Henderson, K.A., Zagorodnov, V.S., Lin, P.-N., Mikhalenko, V.N., Campen, R.K., Bolzan, J.F., Cole-Dai, J., Francou, B., 1998. A 25,000-year tropical climate history from Bolivian ice cores. Science 282, 1858–1864.
Thompson, L.G., Mosley-Thompson, E., Henderson, K.A., 2000. Ice core palaeoclimate records in tropical South America since the last glacial maximum. J. Quat. Sci. 15, 377–394.

Thompson, L.G., Mosley-Thompson, E., Brecher, H., Davis, M., Leon, B., Les, D., Lin, P.N., Mashiotta, T., Mountain, K., 2006. Abrupt tropical climate change: past and present. Proc. Natl. Acad. Sci. U. S. A. 103, 10536–10543.
Thompson, L.G., Mosley-Thompson, E., Davis, M.E., Zagorodnov, V.S., Howat, I.M., Mikhalenko, V.N., Lin, P.-N., 2013. Annually resolved ice core records of tropical climate variability over the past ~1800 years. Science 340, 945–950.
Thouret, J.-C., Finizola, A., Fornari, M., Legeley-Padovani, A., Suni, J., Frechen, M., 2001. Geology of El Misti Volcano near the city of Arequipa, Peru. Geol. Soc. Am. Bull. 113, 1593–1610.
Tillman, P.K., Holzkämper, S., Kuhry, P., Britta, A., Sannel, K., Loader, N.J., Robertson, I., 2010. Stable carbon and oxygen isotopes in *Sphagnum fuscum* peat from subarctic Canada: implications for palaeoclimate studies. Chem. Geol. 270, 216–226.
Treacy, J.M., 1994. Las chacras de Coporaque: andenería y riego en el valle del Colca. IEP, Lima.
Úbeda, J., Palacios, D., Vázquez, L., 2009. Reconstruction of equilibrium line altitudes of Nevado Coropuna Glaciers (Southern Peru) from the Late Pleistocene to the present. Geophys. Res. Abstr. 11. EGU2009-8067-2.
Urrego, D.H., Bush, M.B., Silman, M.R., 2010. A long history of cloud and forest migration from Lake Consuelo, Peru. Quat. Res. 73, 364–373.
USGS, 1998. Certificate of Analysis. Andesite, AGV 2; Basalt, BCR 2. U.S. Geological Survey, Denver.
Valencia, B.G., Urrego, D.H., Silman, M.R., Bush, M.B., 2010. From ice age to modern: a record of landscape change in an Andean cloud forest. J. Biogeogr. 37, 1637–1647.
van der Hammen, T., Santos, A.G. (Eds.), 2003. La Cordillera Central Colombiana transecto Parque Los Nevados. Studies on Tropical Andean Ecosystems, ECOANDES vol. 5. Gebrüder Borntraeger, Berlin.
Van der Putten, N., Mauquoy, D., Vergruggen, C., Björck, S., 2012. Subantarctic peatlands and their potential as palaeoenvironmental and palaeoclimatic archives. Quat. Int. 268, 65–76.
van Geel, B., Renssen, H., 1998. Abrupt climate change around 2,650 BP in North-West Europe: evidence for climatic teleconnections and a tentative explanation. In: Issar, A., Brown, N. (Eds.), Water, Environment and Society in Times of Climatic Change. Kluwer, Dordrecht, pp. 21–41.
Van Geel, E., Buurman, J., Waterbolk, H.T., 1996. Archaeological and palaeoecological indications of an abrupt climate change in The Netherlands, and evidence for climatological teleconnections around 2650 BP. J. Quat. Sci. 11, 451–460.
Vimeux, F., Gallaire, R., Bony, S., Hoffmann, G., Chiang, J., Fuertes, R., 2005. What are the climate controls on isotopic composition (δD) of precipitation in Zongo Valley (Bolivia)? Implications for the Illimani ice core interpretation. Earth Planet. Sci. Lett. 240, 205–220.
Vimeux, F., Ginot, P., Schwikowski, M., Vuille, M., Hoffmann, G., Thompson, L.G., Schotterer, U., 2009. Climate variability during the last 1000 years inferred from Andean ice cores: a review of methodology and recent results. Palaeogeogr. Palaeoclimatol. Palaeoecol. 281, 229–241.
von Post, L., 1946. The prospect for pollen analysis in the study of the earth's climatic history. New Phytol. 45, 193–217.
Vuille, M., Bradley, R.S., 2000. Mean annual temperature trends and their vertical structure in the tropical Andes. Geophys. Res. Lett. 27, 3885–3888.
Vuille, M., Bradley, R.S., Healy, R., Werner, M., Hardy, D.R., Thompson, L.G., Keimig, F., 2003. Modeling $\delta^{18}O$ in precipitation over the tropical Americas: 2. Simulation of the stable isotope signal in Andean ice cores. J. Geophys. Res. 108 (D6), 4175.
Vuille, M., Francou, B., Wagnon, P., Juen, I., Kaser, G., Mark, B.G., Bradley, R.S., 2008. Climate change and tropical Andean glaciers: past, present and future. Earth Sci. Rev. 89 (3), 79–96.
Vuille, M., Burns, S.J., Taylor, B.L., Cruz, F.W., Bird, B.W., Abbott, M.B., Kanner, L.C., Cheng, H., Novello, V.F., 2012. A review of the South America monsoon history as recorded in stable isotope proxies over the past two millennia. Clim. Past 8, 1309–1321.
Walker, M.J.C., Björck, S., Cwynar, L.C., Fisher, D., Long, A., Lowe, J.J., Newnham, R.M., Rasmussen, S.O., 2012. Formal subdivision of the Holocene Series/Epoch: a discussion paper by a Working Group of INTIMATE (Integration of ice-core, marine and terrestrial records) and the Subcommission on Quaternary Stratigraphy (International Commission on Stratigraphy). J. Quat. Sci. 27, 649–659.
Weng, C., Bush, M.B., Chepstow-Lusty, A.J., 2004. Holocene changes of Andean alder (*Alnus acuminata*) in highland Ecuador and Peru. J. Quat. Sci. 19, 685–691.
Weng, C., Bush, M.B., Curtis, J.H., Kolata, A.L., Dillehay, T.D., Binford, M.W., 2006. Deglaciation and Holocene climate change in the western Peruvian Andes. Quat. Res. 66, 87–96.
Williams, J.J., Gosling, W.D., Coe, A.L., Brooks, S.J., Gulliver, P., 2011a. Four thousand years of environmental change and human activity in the Cochabamba Basin, Bolivia. Quat. Res. 76, 58–68.
Williams, J.J., Gosling, W.D., Brooks, S.J., Coe, A.L., Xu, S., 2011b. Vegetation, climate and fire in the eastern Andes (Bolivia) during the last 18,000 years. Palaeogeogr. Palaeoclimatol. Palaeoecol. 312, 115–126.
Zhou, J., Lau, K.-M., 1998. Does a monsoon climate exist over South America? J. Clim. 11, 1020–1040.